NTNU
Norwegian University of Science and Technology
Department of Marine Technology

M.Sc.THESIS

Title:	**Delivered:**
Structural Strength of Work Boats and High Speed Crafts with Pre-fabricated, Floating Panels in Aluminium	21.06.2010
	Availability: Restricted
Student: Toralf Ervik	**Number of pages:** 71 + 7

Abstract:

Aluminium is a material commonly used for smaller boats and high speed crafts due to its low weight. Traditionally the hull construction is performed in a similar manner as that of steel ships, with longitudinal stiffeners fitted through cut-outs in the transverse web frames and welded to the shell plating. This requires much fitting and welding, making the production of hulls a slow and expensive task due to the manual labour needed.

An alternative method for construction of aluminium hulls is to extrude panels consisting of both the shell plating and stiffener. These pre-fabricated panels are then welded directly to the transverse frames, thus reducing the manual labour related to hull production significantly.

This thesis continues the work previously performed by Jon Englund on floating panels. He found that the stresses will increase significantly in a floating frame structure compared to that of a traditional, fixed structure. It was discovered that the main challenge of a floating frame structure is out-of-plane bending stresses occurring in the stiffeners webs due to frame deflections.

By use of finite element analyses and analytical calculations, a compartment of the JumboCat 60 is analysed, and proposals for achieving acceptable stresses are given. The stiffener stresses mentioned above are found to be drastically reduced by increasing the bending- and axial stiffness of the transverse web frames. Local stress concentrations are found in the intersection between stiffener and web frame.

Nonlinear finite element analyses show that substantial strain-hardening can be achieved in the stiffeners webs through cyclic loading. The loss of strength due to welding may thus be partly recovered.

Keyword:

Floating panels. DNV HSLC. Beam theory. Finite element analysis. Cyclic analysis

Advisor:

Jørgen Amdahl

Address:
NTNU
Department of Marine Technology
N-7491 Trondheim

Location
Marinteknisk Senter
O. Nielsens vei 10

Tel. +47 73 595501
Fax +47 73 595697

CONTENTS

LIST OF FIGURES

LIST OF TABLES

LIST OF APPENDICES

1 SCOPE

Konstruksjonsstyrke til bruksbåter og hurtiggående båter med prefabrikerte, utenpåliggende paneler i aluminium

Structural strength of work boats and high speed crafts with pre-fabricated, floating panels in aluminium


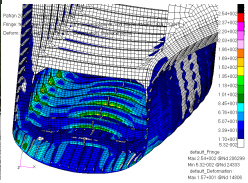

Aluminium er et hyppig brukt materiale for bygging av bruksbåter til oppdrettsnæringen, hurtiggående passasjerbåter og katamaranferger. Produksjon av båtskrog har tradisjonelt krevd mye arbeidsinnsats, med tilpassing av plater, stivere, spant og andre elementer, og et stort omfang av manuell sveising.

I prosjektet ALUBÅT er målsettingen å komme fram til mer kostnadseffektive måter for å produsere aluminiumsskrog til bruksbåter. Det er utviklet konstruksjonsløsninger og bygget mindre båter med utstrakt bruk av prefabrikkerte paneler, bestående av friksjonssveiste ekstruderte aluminiumsprofiler. Panelene er brukt til båtdekk, -sider og -bunn. Med paneler menes her hudplater med ferdige stivere.

En effektiv og økonomisk bruk av panelene i båtbygging forutsetter at panelene kan legges utenpå skott og tverrammer (spant). Dette til forskjell fra tradisjonell bygging av stål- og aluminiumbåter, hvor stivere påsveises platene. Videre føres stiverne normalt gjennom spantene via utsparinger i disse. Stiverstegene sveises normalt til spantene, men det er også eksempler på at de kun sveiste mot spantene i stiverens toppflens, evt. i kombinasjon med brakett for skjæroverføring..

Bruk av prefabrikkerte paneler bestående av ekstruderte profiler sammenføyd med friksjonssveis innfører ingen nye materialkvaliteter i båtbygging. Materialet som brukes er vanligvis aluminiumlegering 6082 i behandling T6, som har godt dokumenterte fasthetsegenskaper. Materialet svekkes ved sveising, men ikke vesensforskjellig fra andre vanlige brukte aluminiumslegeringer og leveringstilstander.

Skrogkonstruksjon med bruk av paneler hvor stiverne legges utenpå skott og tverrammer (spant) krever at det må regnes på mulig styrkereduksjon i kryssingspunktet mellom stivere og skott/tverrammer. Beregningsanvisning for dette er ikke beskrevet i de vanlige dimensjoneringsregler for båter, hverken Nordisk Båtstandard av 1990 for yrkesbåter under 15 m eller Det norske Veritas regler for hurtiggående båter (High Speed, Light Craft and Naval Surface Crafts – HSLC).
For hurtiggående båter aksepteres pr. dato ikke bruk av utenpåliggende paneler.

Det er derfor ansett nødvendig å utvikle modifiserte dimensjoneringsregler for prefabrikkerte paneler. En forutsetning har vært at de modifiserte regler skal ivareta sikkerhetsnivået som er implisitt i dagens regelverk.

Det var umiddelbart ikke klart hvilken dimensjoneringsfilosofi som ligger innbakt i Nordisk Båtstandards krav til platetykkelse og motstandsmoment for stivere. Tilsvarende krav i DnV's Tentative Rules for Certification and Classification of Boats, 1997 og DnV Rules for Classification of High Speed, Light Craft and Naval Surface Craft har derfor også blitt vurdert . Dette arbeidet har bidratt til å avdekke grunnlaget for kravene i Nordisk Båtstandard, og sammenligninger har vist at forskjellene mellom de tre regelverkene er moderate. Når det gjelder yrkesbåter under 15 m har man derfor valgt å foreta modifikasjon av Nordisk Båtstandard, som er den standarden aktuelle byggere av bruksbåter er kjent med. Det har her spesielt blitt sett på kravene til motstansmoment av stivere/spant utsatt for tverrbelastninger.

Styrkereduksjonen på grunn av opplagerkraft (konsentrert kraft) i kryssingspunkt mellom stivere og spant er tatt hensyn til ved at kravet til motstandsmoment økes proporsjonalt med den reduserende virkningen som forårsakes av den konsentrerte opplagerkraften. Det er tatt utgangspunkt i en anerkjent dimensjoneringsprosedyre for kapasitet for plater med konsentrert last på platerand gitt i Eurocode 9.

Et moment som kan ha betydning er evnen utenpåliggende paneler har til å oppta globale skjærkrefter via lastinnføring fra tverrspant. Denne overføringen kan kun skje via sveisen til panelets toppflens mot spant, i motsetning til over hele skipssiden ved tradisjonell utførelse. Globale skrogbelastninger har generelt mindre betydning for (små) bruksbåter og Nordisk Båtstandard inneholder derfor ikke krav til kontroll av global skjærkraft. HSLC har derimot et eksplisitt krav til en slik kontroll ikke minst da tverrspant kan bli utsatt for betydelige dynamiske laster ved høy fart i sjø.

Ved utenpåliggende panel vil ikke panelet bidra med effektiv flens til bøyning av tverrammene. Tverrammene må derfor dimensjoners for å bære lastene som innføres uten medvirking fra huden. Dette gir noe økte dimensjoner på tverrammene, men for øvrig synes det ikke å by på konstruktive utfordringer. Da tøyninger og spenninger i bunnen av tverrammene ikke overføres til huden, vil imidlertid huden få en relativ forskyving i forhold til bunnen av tverrammene. Det medfører en bøyning av stiverstegene i det prefabrikkerte panelet ut av stivestegets plan. I et tidligere arbeid utført av Jon Englund er disse spenningene funnet å være betydelige. Slike bøyespenninger er ikke til å unngå med utenpåliggende panel; spørsmålet er hvor store spenninger som kan aksepteres. HSLC reglene omhandler ikke direkte bruk av slike paneler og de spesielle tøynings- og spenningstilstander som opptrer ved bruk av panel-løsningene, slik at nye vurderinger må utføres.

Hensikten med denne oppgaven er å videreføre arbeidet til Jon Englund. Den vil spesielt fokusere på bøyespenninger ut av stiverstegets plan. Målet for oppgaven er å utarbeide grunnlag for å søke Veritas godkjennelse av en aktuell, planlagt hurtiggående båt fra Fjellstrand med utenpåliggende paneler.

Oppgaven foreslås gjennomført i følgende trinn:

1) Gi en kortfattet beskrivelse av oppbyggingen av aluminiumskrog for bruksbåter og katamaraner, både i tradisjonell utførelse og med bruk av utenpåliggende, prefabrikkerte paneler.

2) Gjennomgang av relevante dimensjoneringskrav for stiver, plater, rammer og skrogbjelke i HSLC, inklusive den foreslåtte modifikasjon av kravet til motstandsmoment av stivere. I den grad kravene kan forstås ut fra enkle betraktninger, skal dette redegjøres for. Det skal også legges vekt på beskrivelse av dimensjonerende laster, med fokus på slamming. Det skal etableres en langtidsfordeling av disse lastene. Så vidt mulig skal fordelingene begrunnes med rasjonelle vurderinger, men det forventes at denne del av arbeidet vil være beheftet med betydelig usikkerhet.

3) Ved hjelp av regneark finne vekt av det prefabrikkerte panelet som funksjon av stiveravstand og rammeavstand med basis i HSLC reglene. Eventuelle beskrankninger, for eksempel med hensyn til platetykkelse, skal tas hensyn til. En vurdering av den relative betydning av fabrikasjonskostnader skal vurderes, blant annet på grunnlag av informasjon fra Fjellstrand AS.

4) Modellere en tverramme eller seksjon av et aktuelt katamaranskrog for analyse med et ikke-lineært elementprogram (ABAQUS). På grunnlag av tegninger stilt til rådighet av Fjellstrand vil en av deres pendelferger (60M JumboCat) bli brukt som eksempel. Modellens utstreking avtales med veiledere. Valg av modellering av randbetingelser skal begrunnes. I den grad tiden tillater kan betydningen ulike stiverproporsjoner studeres.

5) Foreta ikke-lineære sammenbruddsanalyser for modellene utsatt for ytre trykklaster fra normale sjøtrykk og slamming, samt sykliske analyser på grunnlag langtidsfordelingene til lastene. Virkingen av varmepåvirket sone (HAZ) på konstruksjonens motstand vurderes. På grunnlag av disse analysene skal det vurderes hvorvidt utenpåliggende panel har tilfredsstillende motstand mot svikt, både for ekstrem lastpåkjenning eller ved lavsyklus utmatting.

6) Det skal foretas en vurdering av hvorvidt det er behov for å supplere numeriske analyser med laboratorieforsøk.

7) Konklusjoner og forlag til videre arbeid.

Referanser:

Jon Englund: *Structural strength of work botas and high speed crafts with floating frames*, MSc Thesis KTH, Centre for Naval Architecture, Stockholm, December 2009.

Jon Englund: *Oppsummering av FE-analyser på Jumbocat 60 med flytande ramar*, Oma 17.11.2009

Jon Englund: *Finit element-analys av Knut-Johan*, Oma 17.11.2009

Literature studies of specific topics relevant to the thesis work may be included.

The work scope may prove to be larger than initially anticipated. Subject to approval from the supervisors, topics may be deleted from the list above or reduced in extent.

In the thesis the candidate shall present his personal contribution to the resolution of problems within the scope of the thesis work.

Theories and conclusions should be based on mathematical derivations and/or logic reasoning identifying the various steps in the deduction.

The candidate should utilise the existing possibilities for obtaining relevant literature.

Thesis format
The thesis should be organised in a rational manner to give a clear exposition of results, assessments, and conclusions. The text should be brief and to the point, with a clear language. Telegraphic language should be avoided.

The thesis shall contain the following elements: A text defining the scope, preface, list of contents, summary, main body of thesis, conclusions with recommendations for further work, list of symbols and acronyms, references and (optional) appendices. All figures, tables and equations shall be numerated.

The supervisors may require that the candidate, in an early stage of the work, presents a written plan for the completion of the work. The plan should include a budget for the use of computer and laboratory resources which will be charged to the department. Overruns shall be reported to the supervisors.

The original contribution of the candidate and material taken from other sources shall be clearly defined. Work from other sources shall be properly referenced using an acknowledged referencing system.

The report shall be submitted in two copies:
- Signed by the candidate
- The text defining the scope included
- In bound volume(s)
- Drawings and/or computer prints which cannot be bound should be organised in a separate folder.

Thesis supervisor
Prof. Jørgen Amdahl

Contact person at Fjellstrand: Stig Oma

Deadline: June 12??, 2010

Trondheim, January 23, 2010

Jørgen Amdahl

2 SUMMARY AND CONCLUSION

In this thesis various aspects related to the use of floating frame structures in ships have been evaluated from a strength perspective, with a particular focus on the out-of-plane bending stresses in the stiffener webs.

The DNV HSLC rules applicable for fixed structures have been assessed and general modifications are proposed to account for the use of floating frames.

It is found that the transverse web frames need additional strengthening in a floating frame structure compared to a traditional fixed structure, due to the loss of the shell plating as an effective lower flange. A weight increase for the structure seems to be inevitable because of this.

Through finite element analyses and analytical calculations a mid-section compartment of the JumboCat 60 have been evaluated for the symmetrical bottom slamming load condition. Due to the complex geometry of the structure only a limited agreement is achieved between the analytical calculations and the FEA, suggesting that FEA are required to obtain accurate results for the stresses.

The scantlings used for the original, fixed structure have been found to be unsuitable in a floating frame structure, and modified scantlings are proposed for the web frames. The out-of-plane bending stresses in the stiffener webs have been found to depend on the stiffness of the web frames. When replacing the loss of stiffness for the web frames the stiffener stresses are reduced to a near acceptable level.

Nonlinear FEA have shown that there is a potential for strain-hardening in the heat affected areas of the stiffener webs when subjected to cyclic loading. This indicates that stresses exceeding the allowable levels may be tolerated since the elastic stress range will increase.

2.1 Recommendations for Further Work

Original scantlings for the stiffeners are used in the finite element analyses. It is recommended that a new analysis is performed where the local requirements for the shell plating and stiffeners are incorporated. In the new FEA the height of the stiffener webs should be reduced to the actual web height since modelling with shell elements introduces an inaccuracy of the effective height. This reduction in height should also account for the actual radii applied, since they reduce the effective height of the web.

In this thesis the studied load condition is symmetrical bottom slamming. For a full structural analysis intended for class approval all load conditions should be analysed, as given by DNV Classification Notes 30.8.

The FEA with the proposed scantlings showed acceptable overall stresses in the frame, but with local stress concentrations exceeding the allowable stress level. Discussions with DNV are recommended to clear off whether or not these stress concentrations can be accepted.

In this thesis all allowable stress levels include the strength reduction from welding. Since less welding is performed when manufacturing a floating frame structure compared to a traditional fixed structure, this is not necessarily realistic. It should be investigated whether or not the stiffener webs are affected by welding the stiffener flange to the transverse frames. It is possible that the vertical extent of the HAZ is less than the flange thickness, which could open for higher allowable stresses in this area. Due to available time this is not further investigated in this thesis, but experimental tests are recommended.

3 INTRODUCTION

3.1 General

Aluminium is a material commonly used for smaller boats and high speed crafts due to its low weight. Traditionally the hull construction is performed in a similar manner as that of steel ships, with longitudinal stiffeners fitted through cut-outs in the transverse web frames and welded to the shell plating. This requires much fitting and welding, making the production of hulls a slow and expensive task due to the manual labour needed.

An alternative method for construction of aluminium hulls is to extrude panels consisting of both the shell plating and stiffener. These pre-fabricated panels are then welded directly to the transverse frames, thus reducing the manual labour related to hull production significantly. The pre-fabricated panels are commonly referred to as floating panels. An example of a floating panel can be seen in Figure 3.1 below, together with a traditional, fixed structure. This example shows parts of a bottom structure in a transverse view, with the floating panel at the bottom of the figure.

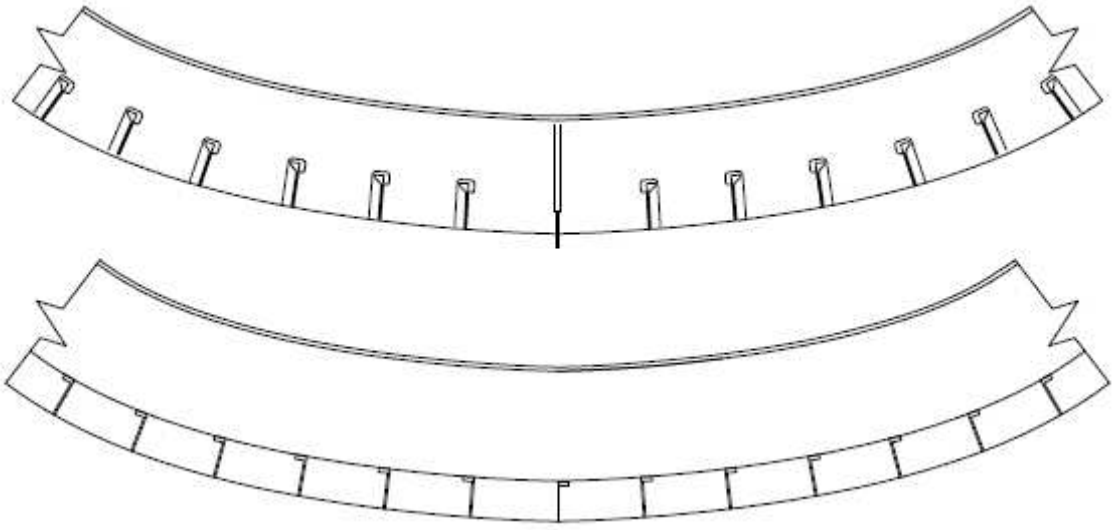

Figure 3.1: Floating panel structure

Ships with pre-fabricated floating panels have previously been built, among others the Norwegian rescue vessel “Knut Johan”. This vessel was inspected in 2006 after sailing for 30 years and showed no signs of damage. (Aalberg, 2006a)

However, since the use of floating panels for ships is not covered by the rules commonly used by Norwegian ship builders a study was performed by Jon Englund in 2009 to evaluate this type of structure from a strength perspective (Englund, 2009a). He performed finite element analyses based on a 60 m car- and passenger high speed catamaran previously built by Fjellstrand AS as a traditional, fixed structure. This vessel is hereby referred to by its type name; JumboCat 60.

Through Englund's master thesis large stresses were found in the structure and it was concluded that there are some issues related to the use of floating frames in ships compared to traditional, fixed structures. The main challenge was highlighted as out-of-plane bending stresses in the stiffener webs, caused by the frame deflections.

The intention of this master thesis is to continue the work performed by Jon Englund, with a particular focus on the stiffener bending stresses mentioned above.

I would like to express my gratitude to Stig Oma at Fjellstrand AS for providing drawings and information of the JumboCat 60, and to my supervisor, Jørgen Amdahl, for guidance and support.

3.2 JumboCat 60

The JumboCat 60 is seen in Figure 3.2 below. It was introduced in 1996 and has since been produced in various versions.

Figure 3.2: JumboCat 60

The following specifications have been provided by Fjellstrand AS and are used in the calculations:

- Length between perpendiculars, Lpp: 54 m
- Breadth moulded, B: 16.5 m
- Vessel speed, V: 35 knots
- Draught, T: 2.24 m
- Displacement fully loaded, Δ: 580 t

In addition, drawings have been given at disposal. These are not included in the thesis for confidentiality reasons.

3.3 Definitions and Abbreviations

DNV	Det Norske Veritas
FEM/FEA	Finite element method/analysis
NLFEA	Nonlinear finite element analysis
DOF	Degree of freedom
m	meter
cm	centimetre
mm	millimetre

4 RULES AND REGULATIONS

Three different sets of rules have previously been evaluated by Jørgen Amdahl as part of the ongoing project "Alubåt", a project sanctioned by The Research Council of Norway to produce methods for reducing the cost of aluminium hull production. (Amdahl, 2006)

-Nordic Boat Standard (NBS) (Norwegian Maritime Directorate, 1990)
-DNV Tentative Rules for Certification and Classification of Boats (DNV, 1997)
-DNV Rules for Classification of High Speed, Light Craft and Naval Surface Craft (HSLC) (DNV, 2005)

The sets of rules above are all intended for traditional ship building, where the frames are welded to the shell plating. For the dimensioning of a floating frame structure some modifications of the present rules are therefore required. This can only be done if the origin of the rules is understood. As NBS and partly also the Tentative Rules are based on simple, empirical rules, the HSLC rules are most suitable as a basis for the dimensioning of a floating frame structure. The HSLC rules are generally recognized as the most advanced of the three sets of rules, and can more easily be interpreted from a strength perspective. Also, the NBS rules are limited to work boats of length less than 15m, and thereby not applicable for this thesis.

In the previous work by Jørgen Amdahl it is also concluded that the different sets of rules can not be combined, since different formulations for the pressure loads are applied. The required dimensions are therefore linked to the calculation of the external loads, and can not be evaluated separately.

The following calculations of the design loads and structural requirements given by DNV HSLC are performed in spread sheets shown in respectively appendix I and II.

4.1 Strength Consequences for Floating Frame Structures

In this chapter the differences between a traditional ship structure and a floating frame structure is discussed from a strength perspective, both generally and more specifically related to the HSLC rules. The structure is split into plating, stiffeners and web frame.

Plating

Jon Englund found that for a floating frame structure the plate stresses are far below the plate stresses for a traditional (fixed) structure, since the shell plating does not act as a flange for the floating frame. However, as he pointed out, this was found for the frame slamming load case, which is commonly not the design load for stiffeners and shell plating.

The dimensioning of stiffeners and plating at the bottom will typically be governed by the local slamming load. For the plate the thickness requirement is based on plate strip theory:

$$t = \frac{22.4 k_r s \sqrt{P_{sl}}}{\sqrt{\sigma_{sl}}} \quad \text{(Sec. 5 - B302)}$$

This is analogous to the moment at the ends of a fixed beam, given as:

$$M_{ends} = \frac{ql^2}{12}$$

For reasons unknown this is twice the moment used for the plate requirement in the DNV Ship Rules, where the moment at the middle of a fixed beam is utilized. If the panels are welded longitudinally midway between two stiffeners it could possibly be allowed to use half the moment, corresponding to the moment in the middle of the plate field. On the other hand future reparations should be accounted for, and at some location the pre-fabricated panels are welded together transversely suggesting that the full moment and the welded properties should be used together.

As seen from the plate requirement formula above there is no beneficial effects to the plate thickness for a floating frame structure.

For the general thickness requirement formula (bending – B202), which may be dimensioning for the shell plating at the sides, there is an aspect ratio term that may increase the required plate thickness for a floating frame structure, since no longitudinal constraint is provided by the frames. However, since the limit for beneficial aspect ratio is s/l<0.5 this term will rarely play a role, and not at all for the JumboCat 60.

The only change to the plate dimensions are related to the different materials used for a fixed and floating frame structure. Since NV-5083 is used for the shell plating in a fixed structure and NV-6082 in a floating frame structure, there will be an increase in the plate thickness requirement. In the welded condition (HAZ) the allowable stresses are respectively 96 MPa and 120 MPa. This gives an increase to the plate thickness of 12%, as shown below.

$$t_{6082} = \sqrt{\frac{120}{96}} * t_{5083} = \underline{1.12 * t_{5083}}$$

It is found that the required thickness for the bottom plating is 6.41 mm.

Stiffener

In a fixed structure the bottom stiffener dimensions are typically governed by the local slamming load. This is mainly the design load for the stiffeners in a floating frame structure also, but some new aspects must also be considered, making the design process more complex.

As analyzed later in this thesis the stiffeners are subjected to out-of-plane bending from the frame deflections in the frame slamming load case. Also, the side stiffeners are subjected to out-of-plane bending by the global forces being transferred from the frames to the shell

plating, through the stiffeners. These effects can not easily be calculated by formulae, and FE analyses are required.

For the local slamming load there are two modifications that must be performed. In a fixed structure some of the pressure forces are transferred directly from the shell plating to the web frames, as illustrated in Figure 4.1. For a floating frame structure this is not the case, and all forces must be transferred through the stiffeners as shear stresses to the web frames. In the formula for required shear area this effect is found in the term (l-s) that reduces the load area.

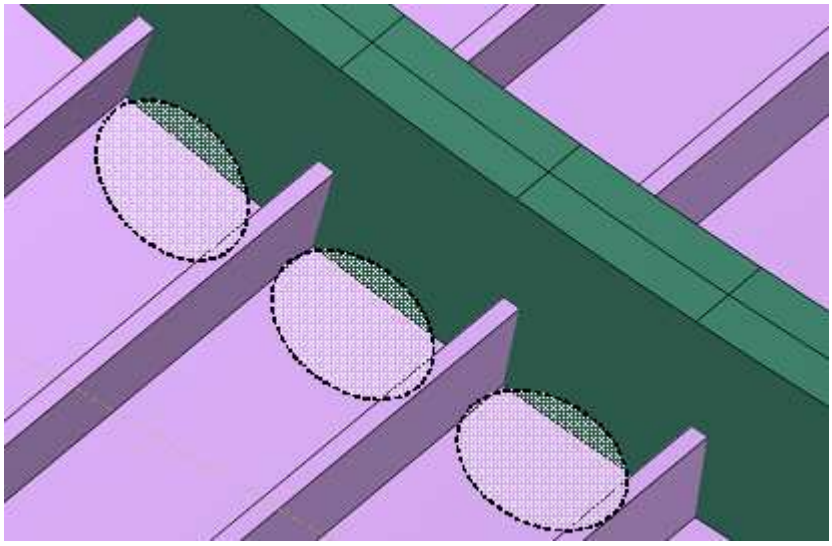

Figure 4.1: Reduced load area for fixed structures

$$A_s = \frac{6.7(l-s)s * P_{sl}}{\tau_{sl}} \text{ (Sec. 5 – C201)}$$

When replacing the term (l-s) with the full frame spacing, l, the required shear area for the bottom stiffeners is increased from 4.2 cm^2 to 5.5 cm^2 (31%) in the specific case of the bottom stiffeners of the JumboCat 60.
It is also seen that the formula above is analogous to beam theory, but with an inherent safety factor of 6.7/5=1.34.

In contrast to the stiffeners in a fixed structure the stiffeners in a floating frame structure may get a reduction in bending capacity due to the concentrated contact force acting in the intersection between stiffener and frame, as illustrated in Figure 4.2 below. The effects of this interaction have been investigated by Arne Aalberg (Aalberg, 2006b) and Jon Englund, including a proposed interaction formula taken from Eurocode 9 (European Committee for Standardisation, 2004). The interaction formula is not further reviewed in this report.

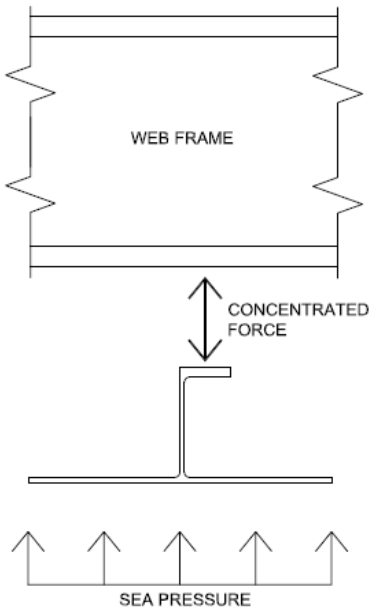

Figure 4.2: Concentrated contact force at intersection

The concentrated contact force may also lead to a nonlinear P-δ effect when combined with the stiffener deflection. An additional moment may thus arise in the stiffener web. However, due to the relatively small deflections it is safely assumed that this effect is marginal, and thus not further reviewed in this thesis.

Web frame

In a traditional ship structure the shell plating acts as a lower flange for both the stiffeners and frames, in addition to carrying the lateral pressure loads. For a floating frame structure this flange is removed for the frames, reducing the stiffness and strength of the frame drastically, as shown in Figure 4.3.

Figure 4.3: Fixed versus floating frame

For the web frame investigated on the JumboCat 60 the inertia moment and lowest section modulus are reduced by respectively 73% and 69% when removing the plate flange. It is a matter for discussion whether the floating frame must completely fulfil the requirements, since the stiffeners will partly add to the bending stiffness of the floating frame. It is however shown later in this thesis that the stiffeners contribution to the frame stiffness is small. It is thus recommended that the loss of stiffness and strength is fully compensated without including the stiffeners.

The strength requirements for web frames in HSLC are section modulus, shear area, and minimum thickness. Except for replacing the loss of section modulus no other modifications are necessary for the web frames.

It must however be noted that the rules for the web frames in HSLC are intended for simple girder systems with regular geometry, where the boundary conditions are easily determined. As this is not the case for large parts of the JumboCat 60 a more direct calculation of the frame system is required.

5 DESIGN CONDITIONS

The studied load case in this report is the Load Condition 2 – "Symmetrical Bottom Slamming", as found in DNV Classification Notes 30.8 (2.3.2) (DNV, 1996) , and illustrated in Figure 5.1.

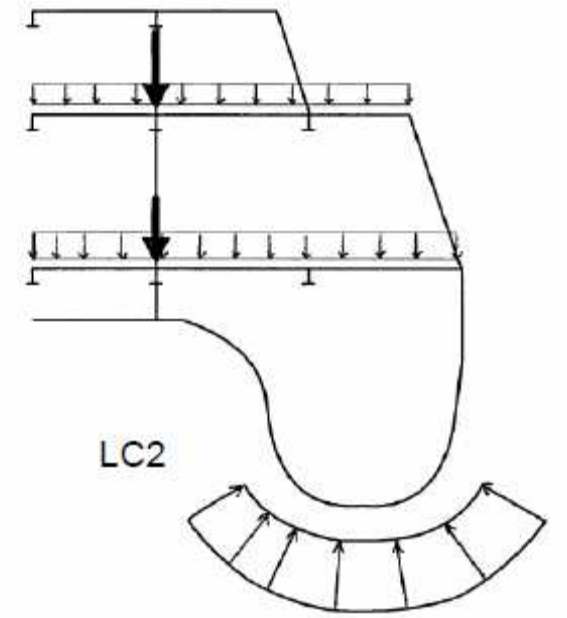

Figure 5.1: Load condition 2 - Symmetrical bottom slamming

The following loads are to be applied for Load Condition 2:

-Slamming pressure on one frame, extending to the upper turn of bilge

-Sea pressure applied on all other frames, extending to the turn of bilge

-Maximum load on decks

5.1 Design Loads

The slamming- and sea pressures are calculated in a spread sheet using the rules in DNV HSLC Pt. 3, Ch. 3.

The design slamming pressure is to be taken as the greater of the "Bottom Slamming" (Section 2 - C201) and the "Pitching Induced Bottom Slamming" (Section 2 – C203). Using the input data given by Fjellstrand AS, the former is found to be the design slamming pressure, with a magnitude of 82.3 kN/m^2. The "Bottom Slamming" pressure is also found to be the greater for the local slamming pressure for plate and stiffener, with a magnitude of 149.7 kN/m^2.

The "Pitching Induced Bottom Slamming" pressure is found to be very sensitive to the lowest service draught at FP, T_L, and would be the design pressure for draughts smaller than 1.88 meters.

The sea pressure is found to vary linearly between 48.5 kN/m^2 at the keel and 32.6 kN/m^2 at the waterline. Since the sea pressure only extends to the upper turn of the bilge in this case, only the maximum value is used.

To verify the spread sheet the pressures outlined above are also found using the software tool "Nauticus Hull – Section Scantlings", which is a rule check software made by DNV.

Both deck loads are taken from the report "Analysis of Transverse Section of the 60m Jumbo Cat" previously performed at Marintek (Økland, 1999). The deck load at the car deck is to be taken as the worst of an evenly distributed pressure and point loads representing the actual wheel loads. Økland found the two load types to give very similar results. The car deck load is therefore taken as an evenly distributed pressure of 4.0 kN/m^2. The passenger deck load is taken as an evenly distributed pressure of 5.35 kN/m^2.

The design loads for Load Condition 2 are summed up in Table 5.1 below.

Table 5.1: Design loads for Load Condition 2

Load component	Pressure [kN/m^2]
Slamming pressure	82.3
Sea pressure	48.5
Car deck pressure	4.0
Passenger deck pressure	5.35

5.2 Design Criteria

The structure consists of two different aluminium alloys:

-Extruded parts: NV-6082 (T6). This includes the shell plating and longitudinal stiffeners
-Cold rolled parts: NV-5083. This includes the transverse frames, brackets and bulkheads

In DNV HSLC the allowable stresses are expressed by the material factor f_1, which vary for different alloys. Also, the material factors are reduced for welded areas, due to softening in the heat affected zones (HAZ).

For aluminium alloys DNV defines the yield strength as 0.2% offset strain, which is not to be taken greater than 70% of the ultimate tensile strength. The reason for this commonly used yield definition is that aluminium alloys have no well defined yield point compared to e.g. mild steel.

The yield stresses and material factors for the two aluminium alloys are shown in Table 5.2 below.

Table 5.2: Material properties

Alloy	Yield stress [MPa]	f_1	f_1 (HAZ)
NV-6082 (T6)	250	0.9	0.48
NV-5083	215	0.89	0.6

Even though not all parts of the structure are affected by welding (HAZ), all allowable stresses in this report will include the strength reduction from welding, as found in DNV HSLC Pt. 3, Ch. 3, Sec. 2 – B400. This is to assure conservatism in the calculations and to account for future reparations and unforeseen changes.

The following allowable stresses are established for dynamic loading in the welded condition, and shown in Table 5.3 below.

Table 5.3: Allowable stresses – dynamic loading (HAZ)

Component	Equivalent stress [MPa]		Bending stress [MPa]		Shear stress [MPa]	
Plating (NV-6082)	$220f_1$	105.6	$200f_1$	96.0	$90f_1$	43.2
Stiffener (NV-6082)	$200f_1$	96.0	$180f_1$	86.4	$90f_1$	43.2
Girder (NV-5083)	$200f_1$	120.0	$180f_1$	108.0	$90f_1$	54.0

Classification Notes 30.8 – 2.6.2 states that the stresses listed above do not refer to local "stress concentrations in the structure or to local modelling deficiencies". No definite value for the allowable peak stress is specified by DNV as these are subject to special consideration in each case.

The out-of-plane bending stresses in the stiffener webs are very local stresses. It is however assumed that these stresses are to be compared with the allowable stresses as given in Table 5.3. This is based on conservatism and should perhaps be discussed with DNV, as the definition of allowable stresses are of great importance in the design process.

Another aspect that preferably should be investigated is whether the stiffener webs are indeed affected by the welding of the stiffener flange, as illustrated in Figure 5.2 below.

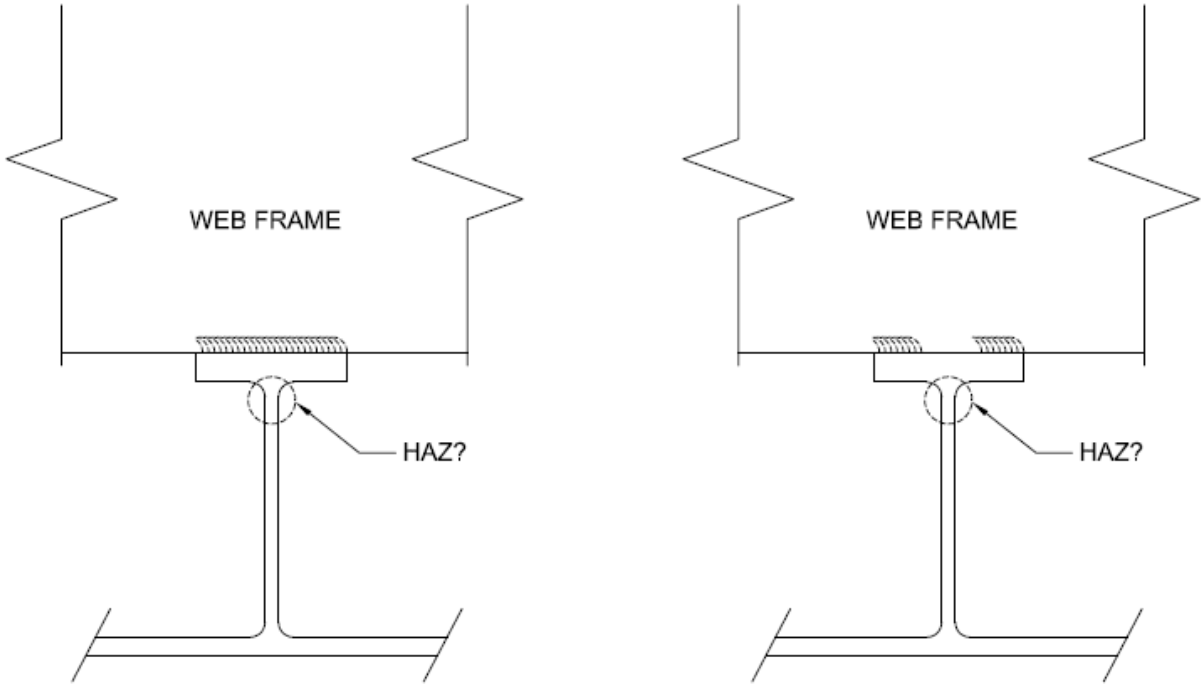

Figure 5.2: Extent of heat affected zones

The heat affected zones are usually defined by the extent to each side of the weld, while the vertical extent is less described. It should be investigated whether or not a thick flange could prevent the HAZ from reaching down to the stiffener webs.

Alternatively it is possible that HAZ in the stiffener web could be avoided by welding only parts of the flange, as shown on the right of the figure above. Discussions with DNV and experiments could clear off these issues. However, due to available time and resources these topics are not further investigated in this thesis.

6 ANALYSIS OF FRAME DEFLECTIONS

In the previous work performed by Jon Englund it is concluded that one of the main challenges with the use of floating frames is the out-of-plane bending stresses occurring in the stiffeners webs due to the frame deflections. It is therefore essential to know the magnitude of the frame deflections, and to keep these as low as reasonably possible.

6.1 Effect of Stiffeners on Frame Deflections

Since the out-of-plane bending stresses in the stiffener webs are caused by the frame deflections it is necessary to establish what effect the stiffeners have on the frame deflections. If this effect is small, the frame deflections and the corresponding stiffener stresses can be calculated without involving the stiffener spacing as a parameter.

In chapters 6.2 and 6.3 the frame deflections are determined by respectively analytical formulae and linear finite element (FE) analyses. The frame deflections are expressed by the vertical deflection at midpoint and the rotational displacements of the frame. The latter can be used more directly to later calculate the stiffener deflection analytically.

6.2 Analytical Calculations of Deflections

The spread sheet used for analytical calculations of the frame is shown in appendix III.

Vertical Deflections

The analytical calculations are based on formulae for vertical deflection at midpoint of a beam and are associated with several uncertainties and simplifications. To transform the problem into a simple statics case the curvature of the structure is ignored. Beneficial shell effects are thus not accounted for, which will give conservative results. The length of the beam in the statics case is taken as the internal width of the hull. Since the boundary conditions are unclear in this case the results are found by taking the average of the fixed and simply supported boundary case. It is not clear whether this will under- or over predict the deflection of the frame. Figure 6.1 illustrates the transformation from the real problem to the two statics cases.

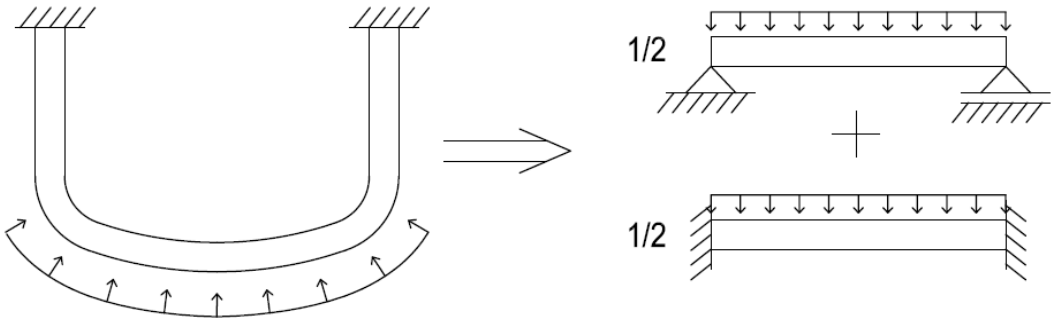

Figure 6.1: Fixed and simply supported boundary conditions

The formulae below are applied for the calculation of deflection at midpoint.

Simply supported:

$$\delta = \delta_{bending} + \delta_{shear} = \frac{5ql^4}{384EI} + \frac{ql^2}{8GA_s}$$

Fixed:

$$\delta = \delta_{bending} + \delta_{shear} = \frac{ql^4}{384EI} + \frac{ql^2}{8GA_s}$$

Rotational Displacement

The calculations of the rotational displacements are associated with the same uncertainties and simplifications as for the vertical deflections. The formula for rotational displacement of a simply supported beam is applied, in combination with a beam length of 2.25 m corresponding to 75% of the internal width of the hull. This way a rough estimate of the rotational displacements can be obtained by the formula below.

$$\beta_{end} = \frac{ql^3}{24EI}$$

6.3 Finite Element Analysis

Three different linear finite element analyses are performed in Abaqus to examine the effect of stiffeners on the frame deflections:

-"Fixed" model: Using the dimensions given by Fjellstrand AS and with the web frame welded to the shell plating (Figure 6.2)
-"Floating frame" model: Using the same dimensions, but with the frame attached only to the stiffener flanges (Figure 6.4)
-"Frame only" model: Same dimensions as the above models, but stiffeners and shell removed (Figure 6.3)

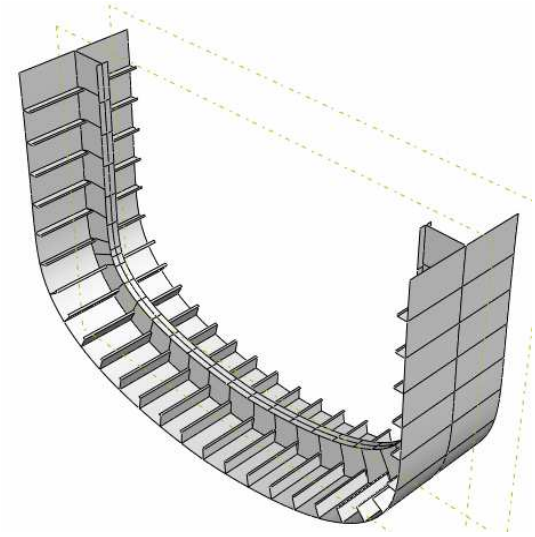

Figure 6.2: "Fixed" model

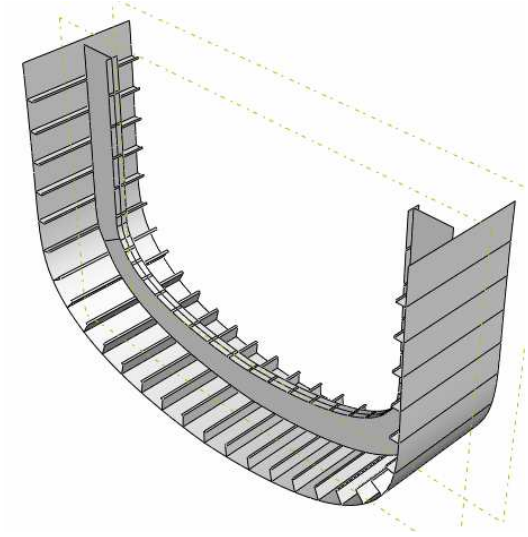

Figure 6.4: "Floating frame" model

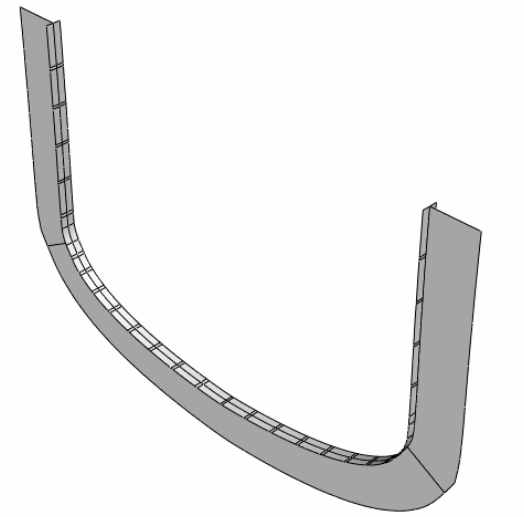

Figure 6.3: "Frame only" model

6.3.1 Modelling

Since the longitudinal stiffeners are bulb-profiles, equivalent L-profiles are used in the models. This is necessary when shell elements are used for modelling. The equivalent L-profiles are optimized with regards to neutral axis and inertia moment, thus giving a good representation of the bulb-profiles for local analyses. The total areas of the L-profiles are slightly larger than the bulb-profiles, which for a global analysis would give non-conservative results. For this analysis it is generally less important, and the error in total area is also less than 1.5% for both profiles. The properties of the two bulb-profiles and equivalent L-profiles are shown in Table 6.1 below.

Table 6.1: Stiffener properties

	"bulb-65"		"bulb-100"	
	Original	**Equivalent**	**Original**	**Equivalent**
Area [mm2]	423.90	430.00	688.10	690.25
Neutral axis [mm]	44.26	44.27	64.67	64.71
Shear area [mm2]	227.50	227.50	450.00	450.00
Ixx [mm4]	1.51E+05	1.51E+05	6.60E+05	6.59E+05
Zx1 [mm3]	3.42E+03	3.41E+03	1.02E+04	1.02E+04
Zx2 [mm3]	7.29E+03	7.28E+03	1.87E+04	1.87E+04

Load

The load used for all three models is the design slamming pressure of 82.3 kN/m2, applied on the bottom structure extending to the upper turn of bilge. For the two first models the load is added as a pressure load on the shell, while for the "frame only" model the load is taken as a line load. Due to the limited extent of these models the deck loads are not accounted for.

Boundary Conditions

Since the objective of this analysis is to examine the relative deflections, only a limited part of the hull is modelled. Longitudinally the models extend 1m, corresponding to one frame spacing. Symmetric boundary conditions are used for the shell/stiffeners in the two first models, corresponding to a case where several frames are subjected to the same pressure. This should give conservative results for the slamming load, since this load does not apply to the neighbouring frames simultaneously.

Vertically the models are ended at the first cross tier, where fixed boundaries are applied. This simplification is reasonable for the slamming load case, since these loads are applied at the bottom of the structure, relatively far away from the boundaries.
To evaluate the stiffeners and frame at the ship side these analyses are not suitable.

Element Mesh

All three models are meshed with the element type S8R, an 8-noded shell element type with reduced integration, and 6 degrees of freedom. Although higher order elements increase the number of DOF drastically compared to linear elements, they also increase the accuracy of the analyses. They are especially suitable for these analyses where it is necessary to recreate the stiffener bending in an exact manner, since quadratic displacements can be reproduced by higher order elements. They are also better than linear elements for curved areas.

All models have an average mesh size of 50 mm, which is more refined than the recommendation from DNV of 3 elements over the web height. The number of elements varies between 1184 and 6993 for the three models, with the fixed model as the largest model. The number of DOF are in the range 23 000 to 128 000.

6.4 Comparison between Analytical Calculations and Finite Element Analysis

Vertical Deflections

The vertical deflection at midpoint found from the finite element analysis and analytical calculations are shown in Table 6.2 below.

Table 6.2: Vertical deflection at midpoint

Model	Finite Element Analysis [mm]	Analytical Calculations [mm]			Englund [mm]
		Fixed	Simply supported	Average	
"Fixed"	6.5	4.2	13.3	8.7	6.9
"Floating frame"	12.4	-	-	-	11.4
"Frame only	14.0	10.5	44.7	27.6	-

The difference in deflection between the "floating frame" model and the "frame only" model is found to be 14% by finite element analysis. It can thus be concluded that the stiffeners only have a small effect on the stiffness of the frame.

Further the results indicate that the boundary conditions correspond to a case far closer to fixed than simply supported boundaries. However, some of the over prediction of the deflections in the analytical calculations may come from the ignored curvature of the frame, which undoubtedly will have a limiting effect on the deflections.

When comparing the deflections found by the finite element analysis with those found by Jon Englund the results seem to agree reasonably well, with differences of respectively 4.5% and 10.5% for the "fixed" and "floating frame" model. This verifies that the simplifications in the analysis are realistic, since Englund performed a more extensive analysis of the deflections by modelling more of the hull.

Rotational Displacement

The maximum rotational displacements found from the finite element analysis and analytical calculations are shown in Table 6.3 below.

Table 6.3: Maximum rotational displacement

Model	Finite Element Analysis [rad]	Analytical Calculations [rad]
"Fixed"	0.0054	0.0051
"Floating frame"	0.0114	-
"Frame only	0.0122	0.0193

Again it is seen that the presence of the stiffeners in the “floating frame” model have little influence on the frame stiffness, as the difference in rotational displacement is 6% between the “floating frame” model and the “frame only” model.

There is a good agreement between the FEA and the analytical calculations for the “fixed” model, while the results for the “frame only” model are more deviant. However, for a rough estimate of a complex structure some deviance is expected. The two maximum rotations in the FEA are found to be 2,18m apart, symmetrically about the centreline, indicating a similarity to the “shortened” simply supported beam used for the analytical calculations.

To illustrate the deformed geometry of the structure, the floating frame model is shown in Figure 6.5 below, with a displacement scale factor of 50.

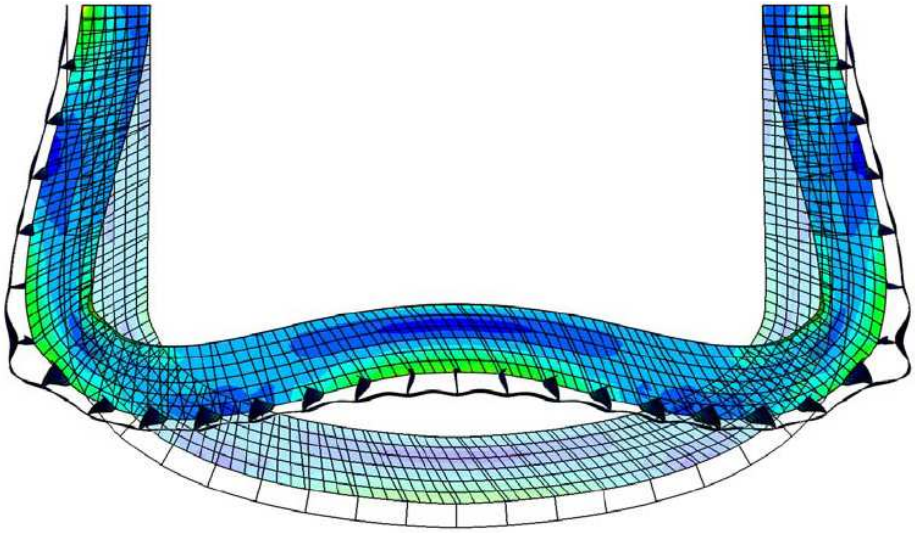

Figure 6.5: Deformed floating frame model

6.5 Possible Solutions for Reducing Frame Deflections

The methods considered for increasing the frame stiffness are discussed below.

1) Fitting pillars between the frame and the cross-tier could be a very effective way of decreasing the frame deflections. The pillar would then act as a support for the frame at midspan. Due to the space available in the engine room this is not possible for the JumboCat 60.

2) A similar solution would be to fit a centre girder between the bulkheads, acting as a support for the frames. However, previous calculations performed by Stig Oma at Fjellstrand AS have shown that the centre girder would need to be very high (1,5-2m) to obtain a sufficiently high stiffness to support the frames, due to a span of 9 m. This centre girder would also need secondary stiffness and thus become both heavy, costly and space demanding.

3) Fitting a flange to the lower edge of the frame would efficiently increase the frame stiffness. Also, the neutral axis would be lowered which again reduces the horizontal deflections of the stiffeners, since these are related to the rotational displacement and the distance to the neutral axis. To reduce the welding time the flange can be fitted on one side of the web instead of the lower edge. This will require some space between the flange and the lower edge, due to necessary welding accessibility.

4) Increasing the area of the top flange would increase the stiffness of the frame. However, for a beam with the neutral axis located as asymmetrically as in this case, the effect will be small. Also, the neutral axis will move upwards, counteracting some of the beneficial effect from the increased inertia moment. Increasing the top flange will be much more effective in combination with a lower flange, as described above.

5) Increasing the height of the frame is an efficient method to increase the frame stiffness, since the Steiner's contribution to the inertia moment contains the distance from the neutral axis squared. However, with an increased height, buckling of the web can become an issue, and more tripping brackets may be necessary. The necessity for tripping brackets is not further investigated in this thesis.

6) Increasing the plate thickness of the web would increase the inertia moment of the frame. This is however not an effective method of increasing the stiffness, since some of the additional cross-sectional area will be located close to the neural axis.

7) Another method for decreasing the frame deflections is to decrease the effective length of the frame by using a larger internal radius of the frame at the bilge. In the formula for rotational displacement the length parameter enters in the third power, suggesting that this may be an effective way of decreasing deflections. Also, since the FE analysis shows that the highest frame stresses occur at the bilge, this method may have an additional beneficial effect by reducing the highest frame stresses.

8) The frame deflections can be reduced by increasing the rotational stiffness of the stiffeners. This will have a limited effect on the deflections with traditional stiffeners, and the increased stiffness would lead to higher stresses in the stiffener webs. A possible solution could be to apply closed profiles, which have a far higher rotational stiffness. This would however produce several new challenges and is not investigated in this thesis.

9) Jon Englund (Englund, 2009b) concluded that a possible solution would be to fit lugs between the stiffeners. This would greatly increase the rotational stiffness of the stiffeners and partly also tie the frame to the shell plate. To achieve acceptable stresses the required frequency of lugs turned out to be very high, thus increasing the welding time drastically.

6.6 Proposed Modifications

As an approach to reduce the frame deflections, a combination of methods 3, 4 and 5 are applied, as illustrated in Figure 6.6 below. The following modifications to the original dimensions are proposed:

- Adding a flat bar 100x15 to the side of the web as a lower flange
- Increasing the height of the web by 50 mm
- Increasing the upper flange from flat bar 100x10 to flat bar 150x15

In addition, the web thickness is decreased by 0.5 mm, since the increased height of the web provides a larger shear area.

The corresponding inertia moment is found to be 113% of the original fixed frame. Since the neutral axis of the frame is located higher than on the original fixed structure the minimum section modulus has moved from the top to the bottom of the frame. The minimum section modulus of the modified floating frame is 124% of the minimum value for original fixed frame, thus satisfying the requirement from DNV.

With the modifications listed above the cross sectional area of the frame is increased by 103%, while the total weight increase for the bottom structure is 24.5%, when the dimensions for shell plating and stiffeners are left unchanged.

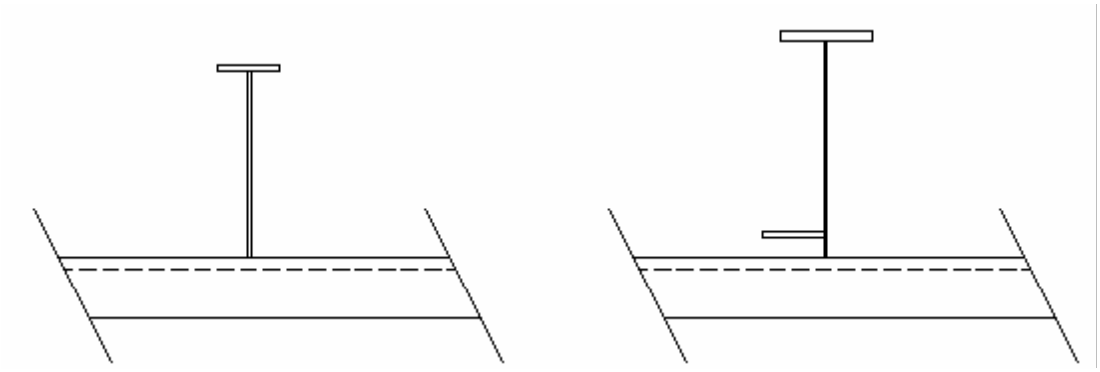

Figure 6.6: Changes to floating web frame

6.6.1 Deflections for Modified Floating Frame Model

A new FE model is created with the modifications stated in chapter 6.6, as seen in Figure 6.7 below.

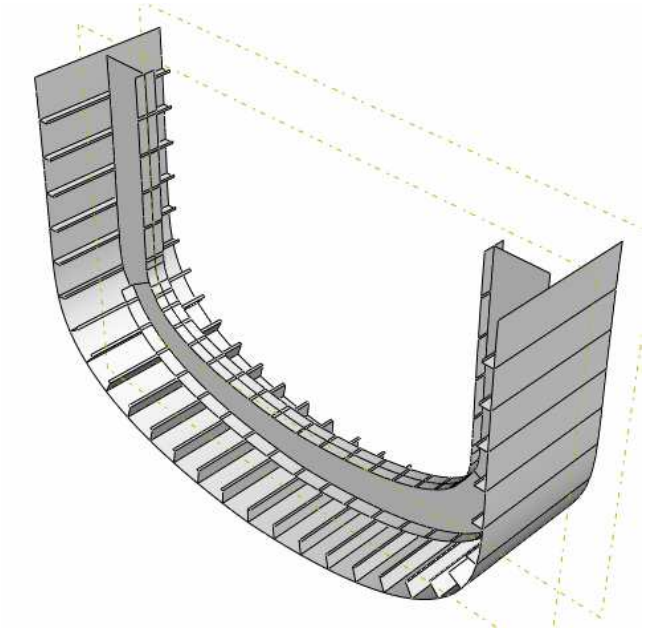

Figure 6.7: "Modified floating frame" model

The results from the analysis of the “modified floating frame” model are presented in Table 6.4 below, with previous results as comparison.

Table 6.4: Frame deflections – vertical and rotational displacements

Model	Finite Element Analysis [mm]	Finite Element Analysis [rad]
“Fixed”	6.5	0.0054
“Floating frame”	12.4	0.0114
“Modified floating frame”	6.2	0.0062

It is seen that the deflections found for the modified floating frame model are close to the deflections found for the “fixed” model, with differences of -6.5% in vertical deflections and +14.8% in rotational displacement. The proposed modifications to the floating frame model are investigated further in the stress analysis in chapter 7.

7 STRESS ANALYSIS OF THE 60M JUMBO CAT WITH FLOATING FRAMES

This chapter aims to evaluate the stresses occurring in the structure when subjected to the loads corresponding to Load Condition 2, as described in chapter 5. Analytical calculations and extended FE analyses are performed. A comparison between the analytical- and FEA results are presented in chapter 7.6, where also the stresses obtained from the simplified FEA described in chapter 6.6.1 are included.

The focus is on stresses in parts of the structure that is not sufficiently covered by the rules in DNV HSLC. This includes the frame structure due to its complex geometry and the out-of-plane bending stresses in the stiffener webs. However, for the extended FE analyses the stresses are reviewed for all parts of the structure, with emphasis on the modified floating frame structure.

7.1 Analytical Calculations of Bending Stresses

The analytical calculations shown in chapter 7.1.1 are based on basic statics formulae for a beam with length 3 meters, while the calculations of the stiffener stresses in chapter 7.1.2 are based on equilibrium equations and the frame deflections found in chapter 6. As for the calculation of the deflections, the boundary conditions are unclear, and the results are found by taking the average of the fixed and simply supported boundary case.

The general formula for stress is shown below.

$$\sigma = \frac{M}{Z} = \frac{M * y}{I}$$

For the traditional fixed frame the neutral axis will generally be closer to the plate than the top flange, and the highest stresses will thus occur in the top flange. For a floating frame structure the situation will be opposite if no lower flange is fitted, making the highest stresses appear at the bottom edge.

7.1.1 Frame Stresses

The following formulae are used for the calculation of the moments.

Fixed boundary conditions:

$$M_{ends} = \frac{ql^2}{12}$$

$$M_{middle} = \frac{ql^2}{24}$$

Simply supported boundary conditions:

$$M_{middle} = \frac{ql^2}{8}$$

The results are shown in Table 7.1 and Table 7.2 below. Compressive stresses are defined as negative values and tensile as positive. The analytical calculations performed here do not differ between the "floating frame" and "frame only" model, since no effect from the stiffeners are accounted for in the calculation of the frame section moduli.

Table 7.1: Bending stresses in frame at midpoint

Model	**Analytical Calculations [MPa]**		
	Fixed	**Simply supported**	**Average**
"Fixed"	-21 / +68	-63 / +205	-42 / +137
"Floating frame"	-219 / +112	-657 / +335	-438 / +223
"Frame only	-219 / +112	-657 / +335	-438 / +223
"Modified floating"	-55 / +39	-166 / +118	-111 / +79

Table 7.2: Bending stresses in frame at ends

Model	**Analytical Calculations [MPa]**		
	Fixed	**Simply supported**	**Average**
"Fixed"	-137 / +42	-	-68 / +21
"Floating frame"	-223 / +438	-	-112 / +219
"Frame only	-223 / +438	-	-112 / +219
"Modified floating"	-79 / +111	-	-39 / +55

7.1.2 Stiffener Stresses

The stiffeners are subjected to two separate loads for the Symmetrical Bottom Slamming load case:

- For the frame slamming load the stiffeners are subjected to both a lateral pressure and the out-of-plane bending caused by the frame deflection.
- For the stiffener slamming load the stiffeners are subjected to a higher lateral pressure, but no additional out-of-plane bending.

For both cases above the stiffeners may get a reduction in bending capacity due to the concentrated contact force acting in the intersection between stiffener and frame, as described in chapter 4.1.

In this chapter only the out-of-plane bending stresses are considered. The stiffeners are separated into bottom stiffeners and side stiffeners in the following chapter. This is done because different effects cause the out-of-plane bending in the stiffeners for the two different areas. The calculations of the stiffener stresses are shown in appendix IV.

Bottom Stiffeners

For the bottom stiffeners the out-of-plane bending is mainly caused by the rotational deflection of the frame when this is subjected to the external slamming pressure. Due to this rotation the lower edge of the frame is displaced horizontally by the rotational angle multiplied by the distance to the neutral axis. Assuming that the shell plate resists this deflection the stiffeners are subjected to a relative out-of-plane displacement.

The relative displacements of the stiffeners are found by:

$$\Delta = \theta * y [mm]$$

The corresponding out-of-plane bending stresses are found by:

$$\sigma = \frac{M}{Z} = \frac{\frac{6EI}{L^2}\Delta}{\frac{I}{y}} = \frac{6E * y * \Delta}{L^2} = \frac{3E * t * \Delta}{L^2} [MPa]$$

Applying the rotational displacements obtained in chapter 6.6.1 the following displacements and stresses are found for the bottom stiffeners.

Table 7.3: Deflections and stresses in bottom stiffeners

Model	**Analytical Calculations**	
	Deflections [mm]	**Stresses [MPa]**
"Floating frame"	2.34	240.9
"Modified floating"	1.31	134.7

The deflections and stresses are drastically reduced for the modified floating frame. This is due to the increased stiffness of the frame, and also the lower location of the neutral axis.

Side Stiffeners

The side stiffeners referred to here are the stiffeners at the outer ship side. Similar derivations can be made for the inner ship side stiffeners, although this would require more simplifications and evaluations because of the more complex geometry.

For the stiffeners at the side the frame bending stiffness has less importance. The main contribution to the out-of-plane bending moments comes from the sea pressure being transferred from the frames to the shell, through the stiffeners. It can also be described as the vertical stiffeners at the ship side acting as springs that balance the global forces.

When neglecting the forces transferred longitudinally to the end bulkheads through the stiffeners the following force equilibrium equation can be established:

$$\Sigma F = \Sigma F_{pressure} - \Sigma F_{deck} - \Sigma F_{stiffeners} = 0$$

$$\Sigma F_{stiffeners} = \Sigma F_{pressure} - \Sigma F_{deck}$$

The spring stiffness of one stiffener is established by setting the displacement, Δ, in the following formula to unity (See also Figure 7.1).

$$V = \frac{12EI}{L^3}\Delta$$

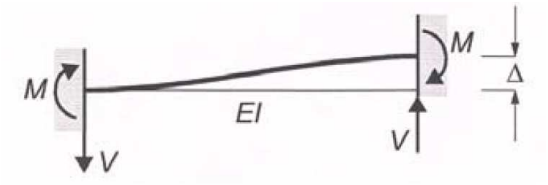

Figure 7.1: Deduction of stiffener spring stiffness

By setting the effective load bearing width to 400 mm and the height of the web to 50 mm, the following spring stiffness is found for one stiffener:

$$k = \frac{12EI}{L^3} = \frac{12 * 70\,000 * \frac{400 * 3.5^3}{12}}{50^3} \approx 9\,600[\frac{N}{mm}]$$

Assuming a homogenous distribution between the stiffeners the total spring stiffness becomes:

$$K_{tot} = 17 * k = 163\,200\,[\frac{N}{mm}]$$

This simplification implies that the frame is perfectly rigid, which of course is incorrect. However, for the stiffeners on average, it is a reasonable simplification.

The unbalanced force is taken as:

$$F_{unb} = \Sigma F_{pressure} - \Sigma F_{deck} = 82.33 * 1500 - (4 * 3000 + 5.35 * 5500)[N]$$
$$\approx \underline{82\,000[N]}$$

Thus giving the average out-of-plane deflection for the side stiffeners as:

$$\Delta = \frac{F_{unb}}{K_{tot}} \approx \underline{\underline{0.50[mm]}}$$

And the corresponding average out-of-plane bending stresses:

$$\sigma = \frac{M}{Z} = \frac{\frac{6EI}{L^2}\Delta}{\frac{I}{y}} = \frac{6E*y*\Delta}{L^2} = \frac{3E*t*\Delta}{L^2} = \frac{3*70\,000*3.5*0.5}{50^2} = \underline{\underline{147[MPa]}}$$

Several simplifications and assumptions are applied in the calculations above. The most important are the effective width of the stiffeners, the simplified rigidity of the frame and the global transfer of the loads.

7.2 Finite Element Analysis

So far in this report only simplified FEA have been presented. However, to get realistic results for the stresses more comprehensive analyses are needed. Three extended models are created, based on the three simplified models “fixed”, “floating frame” and “modified floating”. The larger models are extended both longitudinally and vertically compared to the simplified models, covering a compartment of 9 meters between bulkheads, and extending up to the car deck. All models are prismatic, and will thus exclude possible effects from the double curvature of the structure. The “modified floating” model is shown in Figure 7.2 below, with the deck plate removed for illustration purposes.

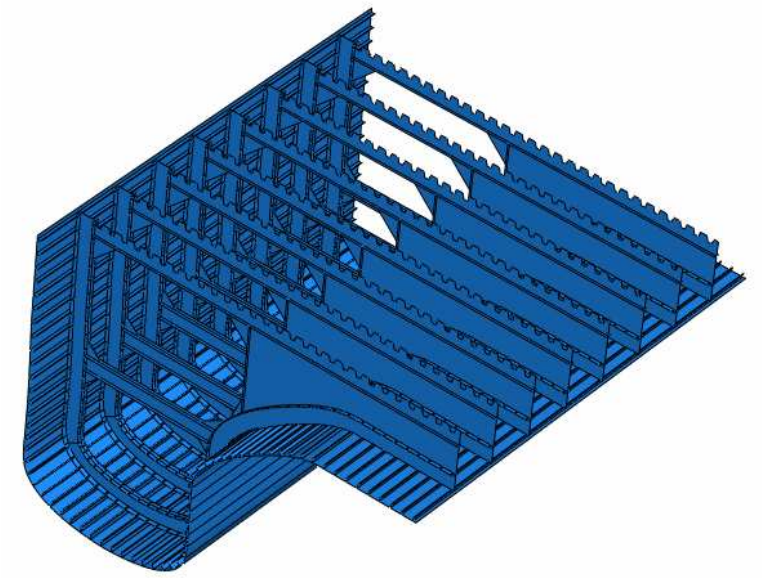

Figure 7.2: Extended finite element model

7.2.1 Modelling

The models are created in Abaqus, and consist of two different parts. The first part includes the shell, stiffeners and deck plate and is made by extruding the cross section imported from AutoCad. The second part includes the frame, flanges, brackets and bulkhead. The frame part is copied longitudinally with frame spacings of 1 meter. To tie the parts together master/slave constraints are established. This is not necessary for the simplified models since they are made as one part.

The bulkheads close to the centreline are in reality stiffened and contain cut-outs. To simplify the modelling the cut-outs are neglected and the stiffeners are "smeared" out over the plate by adding an additional 1.6 mm to the plate thickness. These simplifications have a small influence for the load case in question.

To achieve a smooth structure at the bilge, a stiffener is fitted in the transition with a height corresponding to the average height of the neighbour stiffeners, as illustrated in Figure 7.3 below. This transition was highlighted by Englund and found to give stress concentrations at the bilge due to a sudden change in geometry where the stiffener height changes.

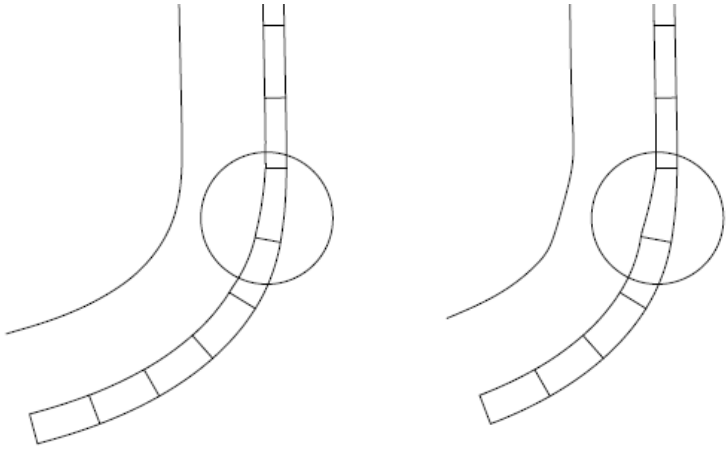

Figure 7.3: Transition stiffener at bilge

Element Mesh

As for the simplified models outlined in chapter 6.3, higher order elements (S8R) are used for the element mesh due to their ability to display quadratic displacements. The average mesh size in general is set to 150 mm, while the frame exposed to slamming is refined to a mesh size of 80 mm. The mesh is finer than that suggested by DNV Classification Notes 30.8, since the purpose is to understand and evaluate the effects of a floating frame structure.

The number of dof are in the range 446 000 to 479 000 for the three models, with the "modified floating" model as the somewhat most heavy.

Boundary Condition

Since both the hull geometry and the loads for the studied case are symmetrical about the vertical plane through the centreline, only one half of the cross section is modelled and symmetry boundary conditions are applied at the centre line.

Longitudinally both ends of the compartment are fixed against displacements and rotations, representing the end bulkheads. According to DNV Classification Notes 30.8 a local model should extend between the middle of two compartments, thus having the bulkhead in the middle of the model. However, for this analysis it is more relevant to analyse an entire compartment since the objective is to study the effect of floating frames. This is also in compliance with the previous work on floating frames carried out by Jon Englund.

Loads

The loads corresponding to Load Condition 2 in DNV Classification Notes 30.8, are applied on the structure, as described in chapter 5.1.

This is the same load condition as previously investigated by Jon Englund. Due to different input data, the values for slamming- and sea pressure are however not identical. The differences are small, with values of respectively +0.5 % and -3%.

A more significant difference between this analysis and the one performed by Jon Englund is the presence of the passenger deck load, as this appears to be excluded from his analyses. Smaller stresses in the stiffener webs at the ship sides are thus expected for this analysis, since less of the force will have to be taken up as a bending moment by the stiffener webs.

Since the models only extend vertically to the car deck, the passenger deck loads are added as point loads at the frames in the ship side, and in the centre. The loads from the passenger deck are assumed to be distributed evenly between the ship sides and centre pillar. Due to the symmetric boundary conditions at the centreline 1/3 of the passenger deck load is added to the sides, while 1/6 is added in the centre. Even though there are no pillars at each frame, the pillar loads from the passenger deck are evenly distributed between the frames in the model, due to the longitudinal bulkhead in the centre.

The loads applied on the structure are illustrated in Figure 7.4 below, with the omitted parts of the cross section shown as dashed lines.

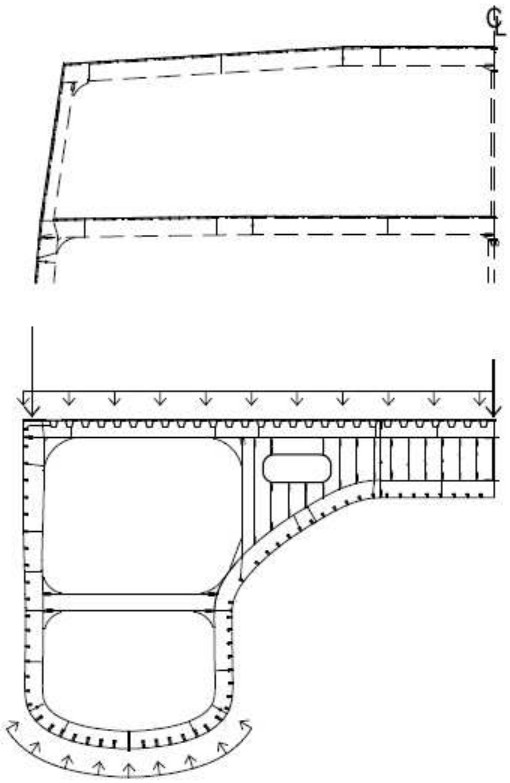

Figure 7.4: Applied loads

7.3 Original Floating Frame

The results from the FE analysis of the floating frame model with original scantlings are shown in chapters 7.3.1 and 7.3.2 for respectively frame stress and stiffener stress.

7.3.1 Frame Stress

The equivalent (von Mises) stresses for the web frame of the original floating frame model are shown in Figure 7.5 below. Only the bottom part of the frame subjected to the slamming pressure is shown due to low stresses in the top part and surrounding frames. A deformation scale of 50 is applied.

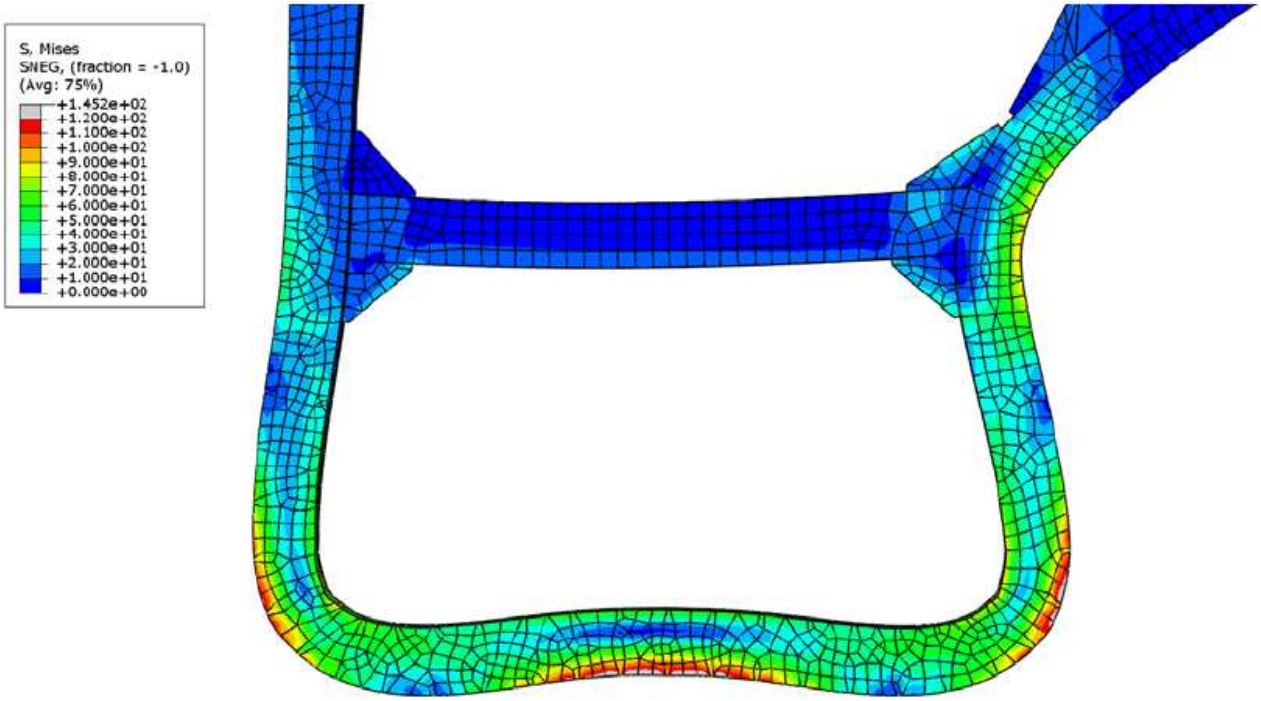

Figure 7.5: Equivalent stress in web frame (original floating)

Large parts of the structure have equivalent stresses exceeding the allowable stresses of 120 MPa. The highest stress is found at the upper edge of the bilge, with a value of 145 MPa. In addition to the upper edge of the bilge, also the lower edge of the bilge and the middle span display high stresses. Although there are some local stress concentrations, the stresses are in general nominal bending stresses and can not be disregarded. The highest stress in the middle of the bottom frame is found at the lower edge, demonstrating the effect of having the neutral axis located close to the flange.

The bending stresses are found to exceed the allowable stress in the same three areas, with an extreme value of -155 MPa at the middle span (bottom edge). Due to higher stress values and lower allowable stresses, bending is even more critical than the equivalent stresses.

As shown in Figure 7.6 below, the shear stresses are mainly within the allowable limit of 54 MPa. The only area exceeding the allowable stress is found at the bilge with a value of 57 MPa. However, this is only in a very local area and should therefore be evaluated specially by DNV.

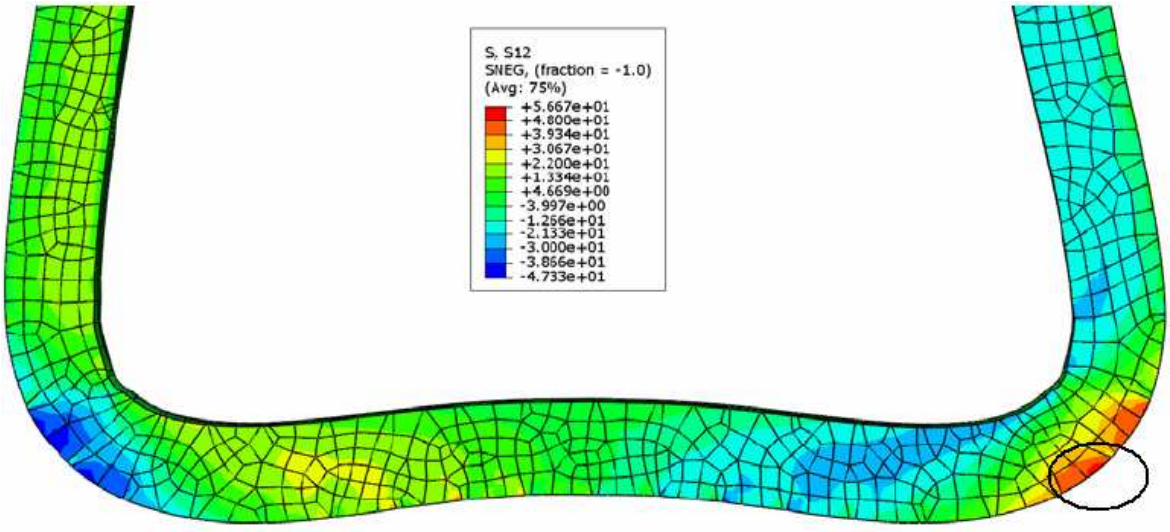

Figure 7.6: Shear stress in web frame (original floating)

7.3.2 Stiffener Stress

Since the studied load case in this analysis is the frame bottom slamming only the out-of-plane bending stresses are presented in this chapter. For shear stresses and longitudinal bending stresses the local stiffener slamming pressure would be the design load, which is not covered here.

The results are split into three geometrical regions, with the stiffeners exceeding the allowable stress level marked in Figure 7.7 below.

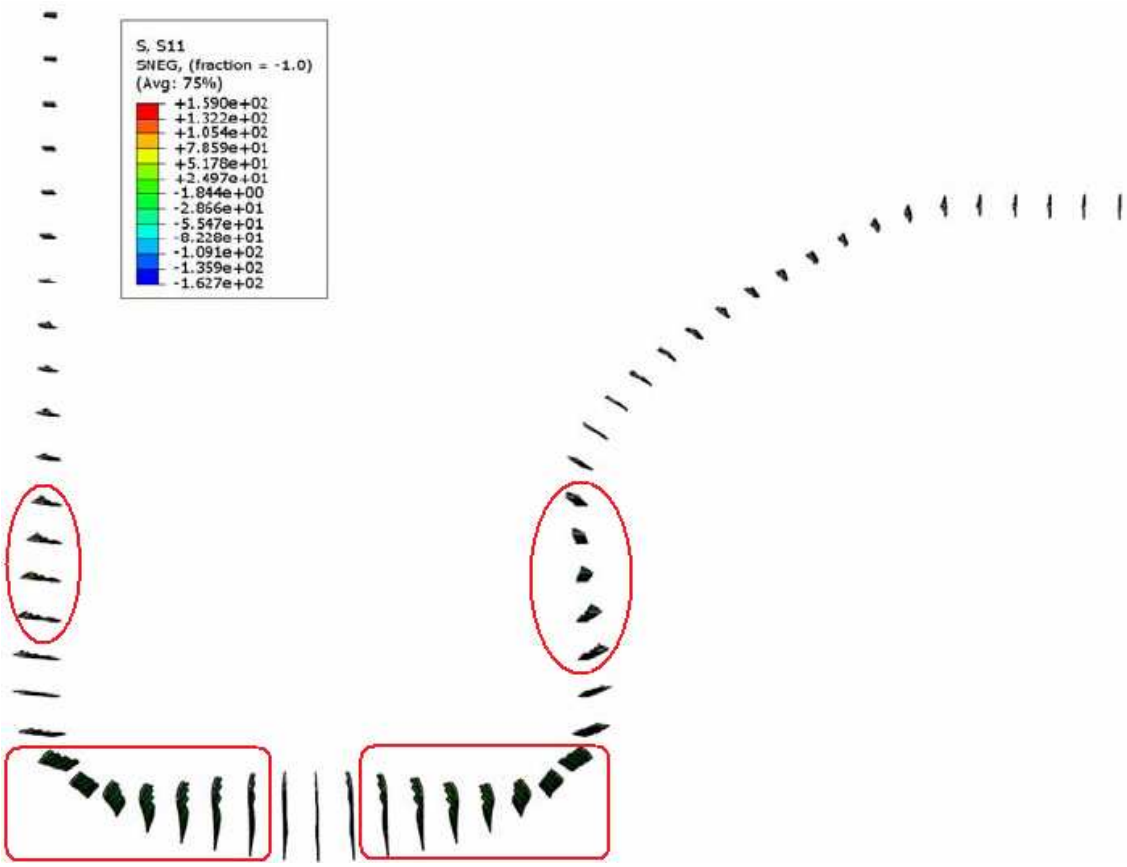

Figure 7.7: Stiffeners exceeding the allowable stresses (original floating)

Outer side stiffeners
The allowable bending stress of 86.4 MPa is exceeded by four stiffeners, with values ranging from 99 MPa to 144 MPa.

Bottom stiffeners
Due to the large rotation of the web frame all stiffeners except for the three middle stiffeners display stresses above the allowable limit, with an extreme value of 163 MPa.

Inner side stiffeners
Stresses of 87-147 MPa are observed in five stiffeners.

The allowable stresses are exceeded by 21 stiffeners in total, with a maximum value of 189% compared to the allowable stress. It is found that the bottom region is the most critical, although the side stiffeners at both sides also exceed the allowable stress.

7.4 Modified Floating Frame

The results from the FE analysis of the modified floating frame model are shown in chapters 7.4.1 and 7.4.2 for respectively frame stress and stiffener stress.

7.4.1 Frame Stress

The equivalent stress for the web frame of the modified floating frame model is shown in Figure 7.8 below. The lower flange is removed from the plot for illustration purposes and a deformation scale of 50 is applied.

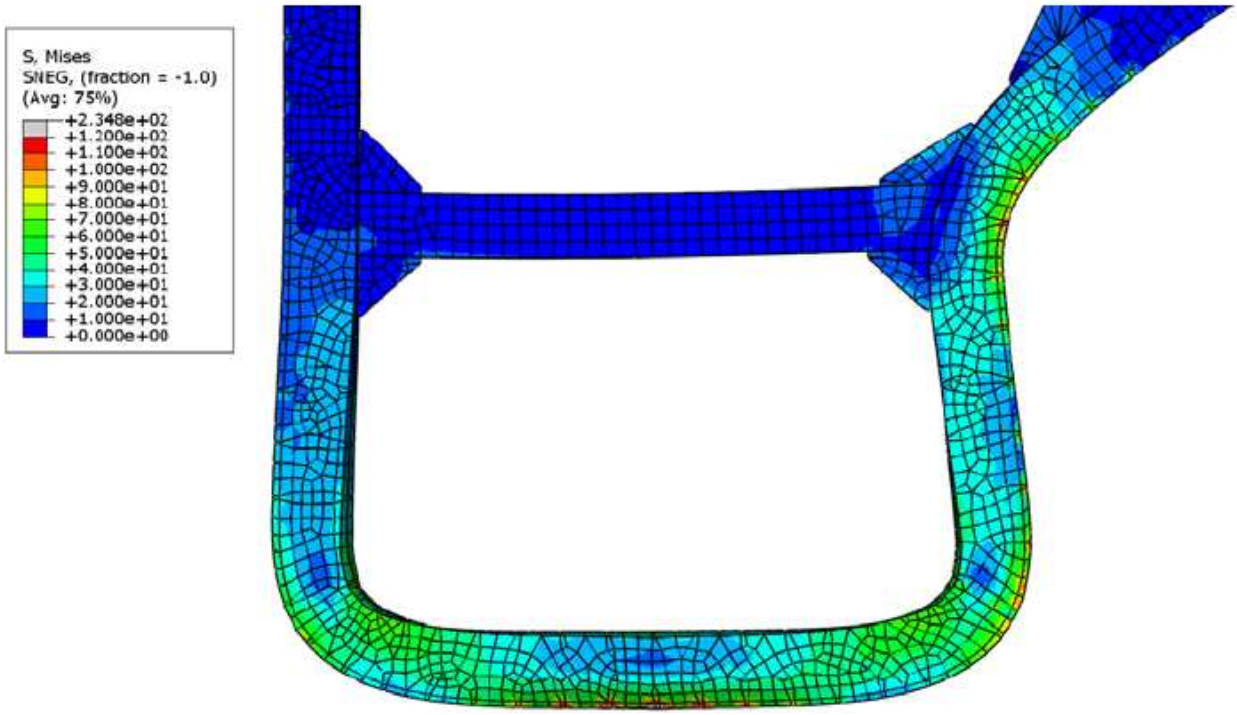

Figure 7.8: Equivalent stress in web frame (modified floating)

It is found that several areas in the frame exceed the allowable stresses of 120 MPa given by the rules, and an extreme value of 235 MPa is found. However, all stresses above 120 MPa are very local, and thus not comparable to this criterion. The extreme value of 235 MPa can be disregarded altogether as it appears to be a model deficiency, as seen in Figure 7.9 below.

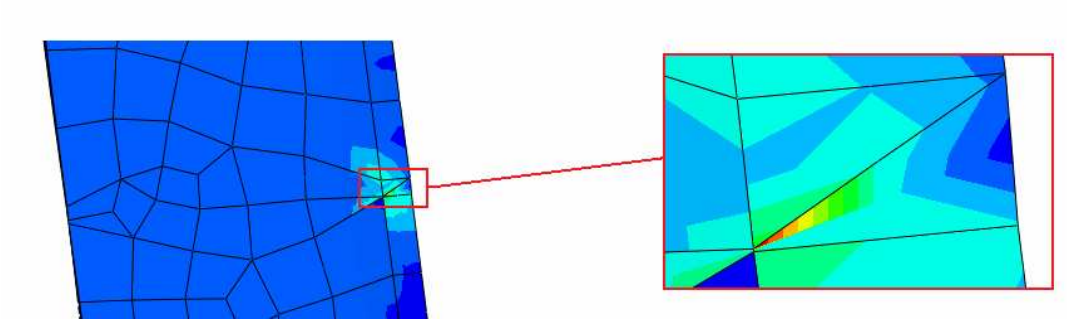

Figure 7.9: Modelling deficiency

When disregarding this modelling error there are still other local stress concentrations of values 160-190 MPa in the model. Common for all the stress concentrations is that they are located in the intersections between stiffener flange and frame, as shown in Figure 7.10 below.

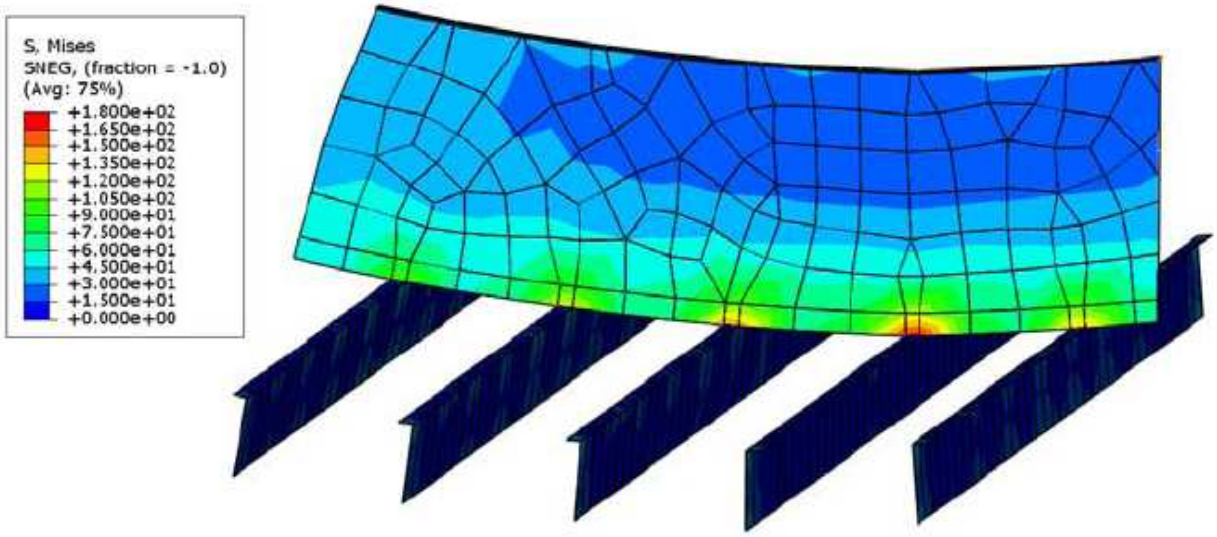

Figure 7.10: Stress concentrations at intersection

As stated in DNV Classification Notes 30.8 (2.6.4) the local stress concentrations are subject to special consideration in each case. The local peak stresses are likely to depend on the width and thickness of the stiffener flanges, and the web thickness of the frame. It should be cleared off with DNV whether or not these local stresses can be tolerated.

When neglecting the local stress concentrations the highest stress is found at the inner edge of the bilge with a value of 119 MPa, thus still fulfilling the requirement for equivalent stresses. The highest overall equivalent stresses are 70-80 MPa, as seen in Figure 7.8.

Both the overall bending stresses and the shear stresses are within the allowable limits for the entire structure.

7.4.2 Stiffener Stress

The results of the stiffener stresses are split into three geometrical regions, with the stiffeners exceeding the allowable stress level highlighted in Figure 7.11 below.

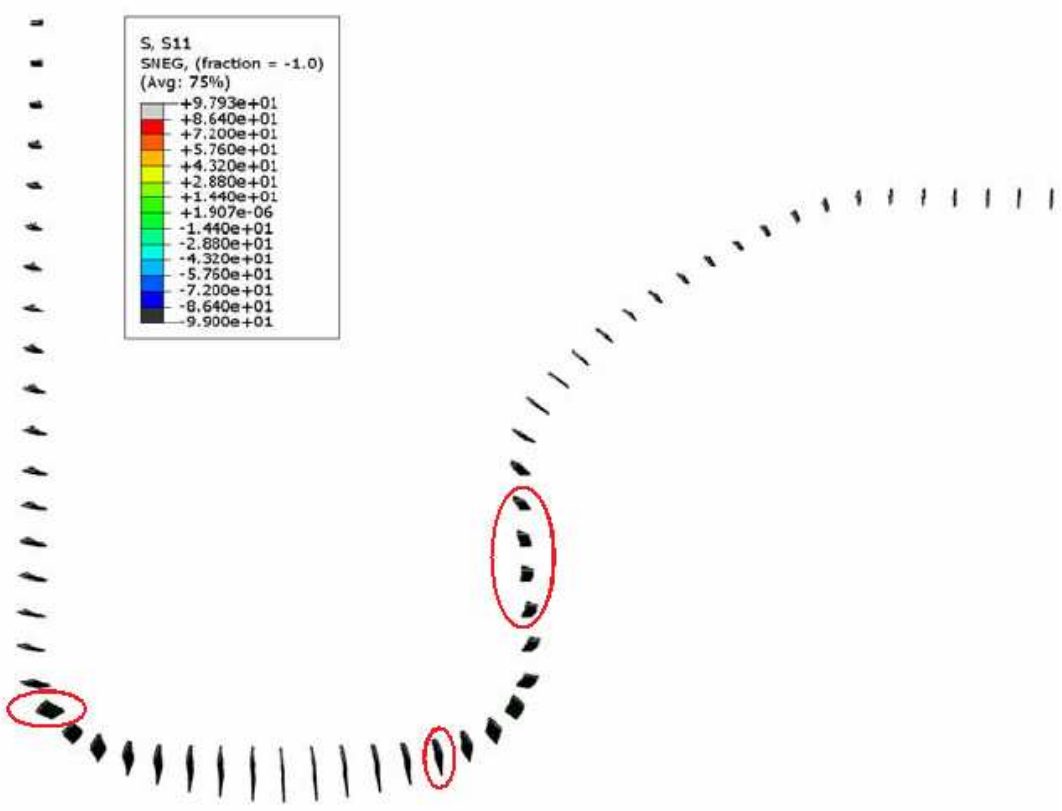

Figure 7.11: Stiffeners exceeding the allowable stresses (modified floating)

Outer side stiffeners
The highest bending stress is found to be 70 MPa, with no areas above the allowable stress level.

Bottom stiffeners
Two stiffeners exceed the allowable stress level of 86.4 MPa. These are found close to the bilge, at each side, with values of 99 MPa and 89 MPa.

Inner side stiffeners
Four stiffeners exceed the allowable stress, with values ranging from 85 MPa to 99 MPa

The stress levels in the stiffeners are above the allowable levels given by DNV for six stiffeners, with the inner side as the most critical region. Stress values of 115% of the allowable are observed in two stiffeners.

7.5 Effect of Modifications

The modifications referred to in this chapter are explained in chapter 6.6.

The modified web frame has a section modulus slightly greater than the traditional, fixed structure and fulfils the requirements of section modulus from DNV. This ensures acceptable overall bending stresses, which are reduced from 155 MPa in the original floating model to 75 MPa in the modified. However, since the stiffness of the frame increases drastically, high local stresses are obtained in the intersection between frame and stiffener. These local stresses are not present in the original model, since the frame is less rigid and a softer connection is ensured.

The stresses in the stiffeners are closely related to the deformed geometry of the structure. The deformations are shown for the two models in Figure 7.12 below, with a deformation scale factor of 100.

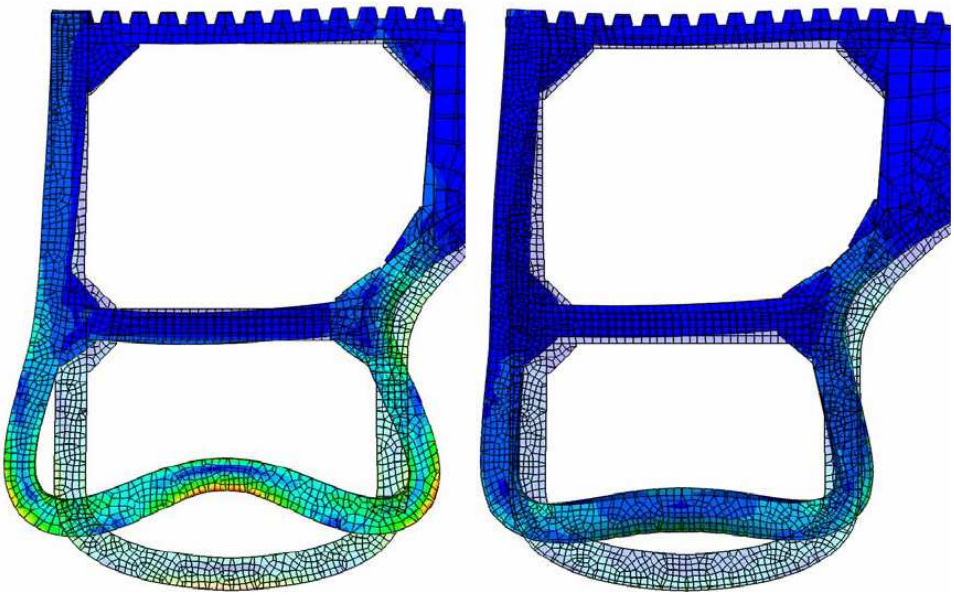

Figure 7.12: Deformed models (original - left, modified - right)

It is seen that the rotational deformations are much larger for the original model, causing large out-of-plane bending stresses in the stiffener webs. For the stiffer modified frame the rotations are decreased drastically, and the highest stiffener bending stress is reduced from 163 MPa to 99 MPa.

While the decreased stresses for the bottom stiffeners can be ascribed solely to the decreased rotations, there is one more aspect to the side stiffeners. In addition to the rotations almost vanishing at the sides for the modified model, the axial stiffness is also increased. This causes the forces from the bottom to be transferred to the shell through the stiffeners in a more uniform manner, meaning that more stiffeners are able to contribute to the resistance. For the original model, however, only a few stiffeners contribute due to the low axial stiffness of the frame. The same stiffeners are in addition subjected to bending, thus increasing the stresses further.

There is no doubt that the original scantlings are unsuitable for a floating frame structure, due to high stresses in both frames and stiffeners. When modifying the scantlings of the transverse web frames the stresses are reduced significantly for the frame itself, and also for the stiffeners.

Acceptable stress levels are obtained for large parts of the structure, with exception to local stresses in the web frame and bending stresses in some of the longitudinal stiffeners. It is possible that the stress concentrations in the frame can be accepted by DNV, due to the local nature of these stresses, which opens for an exception of the allowable stress levels. The fine, quadratic mesh applied can also be a reason to accept these local stress concentrations.

The out-of-plane bending stresses in the stiffeners are very local in the longitudinal direction, but they are still pure bending stresses and can most likely not be disregarded. However, since the stresses are local it might be possible to avoid heat affected zones in way of the largest stresses. This would increase the allowable stresses beyond the actual stress level in the structure.

7.5.1 Effect of Passenger Deck Load

The FE analyses discussed in this chapter include the passenger deck loads previously discussed in chapter 7.2.1. These loads are assumed to give lower stiffener stresses by bringing the structure closer to equilibrium with regards to forces. To confirm this assumption, which also the analytical calculations are based on, the FE analysis of the modified floating frame is repeated with the passenger deck loads excluded.

At the outer side the stiffener stresses are found to increase from 70 MPa to 100 MPa, and a total of nine stiffeners exceed the allowable stresses. Increase of stresses are also observed for the inner side stiffeners, although not as dramatic as for the outer side stiffeners. The largest bending stress is found to increase from 99 MPa to 105 MPa, and five stiffeners are above the allowable level. No practical difference is observed for the bottom stiffeners.

The out-of-plane bending stresses in the side stiffeners are found to increase when the passenger deck loads are omitted, thus confirming the basis of the analytical calculations. The effect is by far most pronounced at the outer side, since the forces are transferred through the stiffeners to the shell plating in this region.

7.6 Comparison between Analytical Calculations and Finite Element Analyses

The results from the three different analyses are presented in tabulated form in this chapter.

7.6.1 Frame Stress

The bending stresses at midpoint and ends of the web frame are shown in Table 7.4 and

Table *7.5* below. For the FEA results only the nominal bending stresses are presented. The local stress concentrations are omitted, although it can be difficult to separate these in some areas.

Table 7.4: Comparison of bending stresses in frame at midpoint

Model	Extended FEA [MPa]	Simplified FEA [MPa]	Analytical Calculations [MPa]		
			Fixed	Simply supported	Average
"Fixed"	-15 / +60	-40 / +90	-21 / +68	-63 / +205	-42 / +137
"Floating frame"	-155 / +75	-210 / +100	-219 / +112	-657 / +335	-438 / +223
"Frame only	-	-230 / +90	-219 / +112	-657 / +335	-438 / +223
"Modified floating"	-55 / +30	-100 / + 50	-55 / +39	-166 / +118	-111 / +79

Table 7.5: Comparison of bending stresses in frame at ends

Model	Extended FEA [MPa]	Simplified FEA [MPa]	Analytical Calculations [MPa]		
			Fixed	Simply supported	Average
"Fixed"	-70 / +20	-80 / +30	-137 / +42	-	-68 / +21
"Floating frame"	-130 / +40	-210 / +100	-223 / +438	-	-112 / +219
"Frame only	-	-170 / +40	-223 / +438	-	-112 / +219
"Modified floating"	-30 / +40	-60 / + 90	-79 / +111	-	-39 / +55

It is seen in the tables above that both the simplified FEA and the analytical calculations over predict the stresses in the frame. Some of this can be ascribed to the longitudinal effect in the extended FEA, where loads are transferred from the frame subjected to the high slamming load to the neighbouring frames that are less loaded. This effect is not accounted for in the simplified FEA and the analytical calculations, as these assume a uniform load due to symmetric boundaries.

For the stresses at midpoint there seem to be some consistency between the analytical calculations and the finite element analyses. The extended FEA agree well with the analytical calculations obtained for fixed boundaries, while the simplified FEA correspond better with the averaged boundaries. It appears that the boundary conditions in reality are closer to fixed than simply supported.

Less consistency is found in the results at the ends. This can partly be caused by the complex geometry and the fact that it is difficult to determine the bending stresses from FEA in an exact manner due to large stress variations.

7.6.2 Stiffener Stress

The tabulated results for the stiffener bending stresses are presented in Table 7.6 and Table 7.7 below. For the analytical calculation of the side stiffeners the results are identical for the floating and modified frame since the axial stiffness of the frame is neglected.

Table 7.6: Comparison of bending stresses in bottom stiffeners

Model	Extended FEA		Simplified FEA		Analytical Calculations	
	Deflection [mm]	Stress [MPa]	Deflection [mm]	Stress [MPa]	Deflection [mm]	Stress [MPa]
"Floating frame"	1.29	162.7	1.74	246.3	2.42	249.0
"Modified floating"	0.70	99.0	1.05	197.8	1.31	134.7

Table 7.7: Comparison of bending stresses in side stiffeners

Model	Extended FEA		Simplified FEA		Analytical Calculations	
	Deflection [mm]	Stress [MPa]	Deflection [mm]	Stress [MPa]	Deflection [mm]	Stress [MPa]
"Floating frame"	0.83	144.5	1.03	191.6	0.50	147.7
"Modified floating"	0.59	70.4	0.66	111.0	0.50	147.7

It is seen that the stresses are over predicted by the simplified FEA and the analytical calculations for both analyses, compared to the extended finite element analysis. This is due to longitudinal transfer of forces being accounted for in the extended FEA.

For the finite element analyses there seem to be some inconsistency between the deflections and stresses, compared to the simple beam theory utilized in the analytical calculations. This can be caused by rotations of the shell plating and stiffener flange, since the analytical formula assumes these faces to remain normal to the stiffener web after deflecting. Another aspect is how the stresses are interpreted in the FE analyses, since some of the stresses may come from compression in addition to the pure bending contribution.

Since the FE models are made of shell elements with no thickness, the effective height of the stiffener webs are not completely correct. When modelling with shell elements the plating and flange are located at their neutral axis (middle) to achieve the correct section modulus about the strong axis, see Figure 7.13 below.

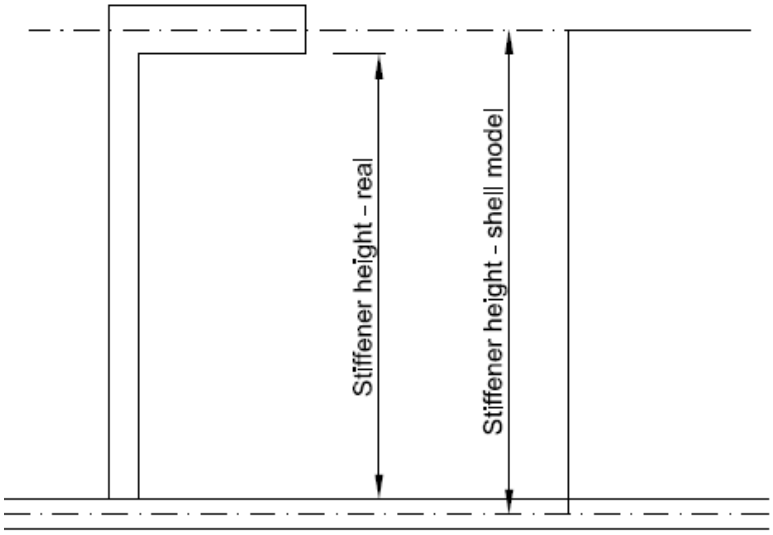

Figure 7.13: Inaccuracy for shell element model

This modelling procedure gives correct results for most analysis, but introduces an inaccuracy in this analysis since the effective height of the stiffener web is important for the out-of-plane bending. The inaccuracy is amplified by the fact that the real stiffeners would contain radii that would reduce the real effective height further.

Although decreasing the stiffener height of the shell model would underestimate the section modulus, it would perhaps give the overall best results for this kind of analysis.

8 EFFECT OF RADIUS FOR EXTRUDED PROFILES

Changes in geometry over a cross-section are often associated with large stress concentrations, which may lead to local yielding and fractures. In the case of extruded panels with stiffeners, the corner radii can be chosen more freely than what is the case in traditional ship building, where the stiffeners are welded to the plate. It is therefore relevant to study what effect the corner radii have on the stress concentration occurring in the corners of a stiffener subjected to out-of-plane bending.

The study is based on the T-profile "T88x5x50x10" with dimensions W78x5 / FL50x10 [mm] and original radii of 5 mm. By altering the radii, the peak stresses are found for radii of 1-8 mm. In addition to the stiffener a plate of thickness 6 mm is included in the model. The same radii are used between the web and plate as for the web and flange connection. The model with radii of 1 mm is shown in Figure 8.1 below.

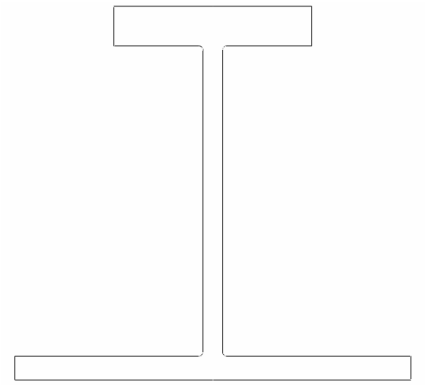

Figure 8.1: Cross section

The horizontal displacement is set to 1 mm in all the calculations.

8.1 Analytical Calculations

The out-of-plane bending case for the stiffener is equivalent with a beam subjected to translation while fixed against rotation. This case is shown in Figure 8.2 below.

Figure 8.2: Out-of-plane bending

The formula for the corresponding moment is:

$$M = \frac{6EI}{L^2}\Delta$$

Since the objective of the analysis is to study various radii, a reduction of length depending on the radii is needed to establish the effective length of the beam. This reduction is taken from DNV HSLC Pt3,Ch3, sec1, I 101, where it is stated that the two thirds of the radius is to be deducted from the effective span, as shown in Figure 8.3 below. The length reduction taken from DNV is normally applied for beams, but in this case the stiffener is regarded as a beam by strip theory.

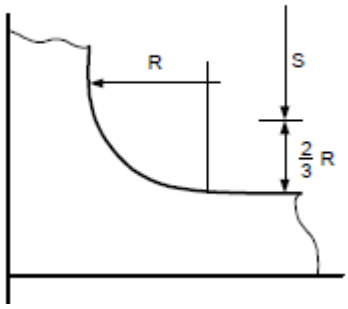

Figure 8.3: Effective span of a beam

By applying the formulas above the nominal bending stresses for the radii of 1-8 mm are calculated in a spread sheet. Stress concentrations are omitted from the analytical calculations altogether.

8.2 Finite Element Analysis

Two-dimensional models are created in Abaqus, with the element type CPS8R. This is an 8-noded, plane stress element, with reduced integration. A fine mesh is created with average element size of 1x1 mm.

The lower edge of the plate is fixed against translation and displacements, while the upper edge of the flange is given a prescribed displacement of 1 mm horizontally.

8.3 Results

The results are summed up in Table 8.1 and Figure 8.4 below. The analytical results are nominal bending stresses, while the FE results are peak stresses.

Table 8.1: Stresses in web for various radii

Radii [mm]	FEA – Bending [MPa]	FEA – vonMises [MPa]	Analytical – Bending [MPa]
1	201.1	202.8	178.6
2	190.3	190.6	185.0
3	181.1	183.5	191.7
3,5	*180.9*	*180.4*	*195.3*
4	181.6	183.4	198.8
5	183.3	186.2	206.3
6	188.0	189.8	214.3
7	192.2	194.4	222.7
8	197.6	200.1	231.6

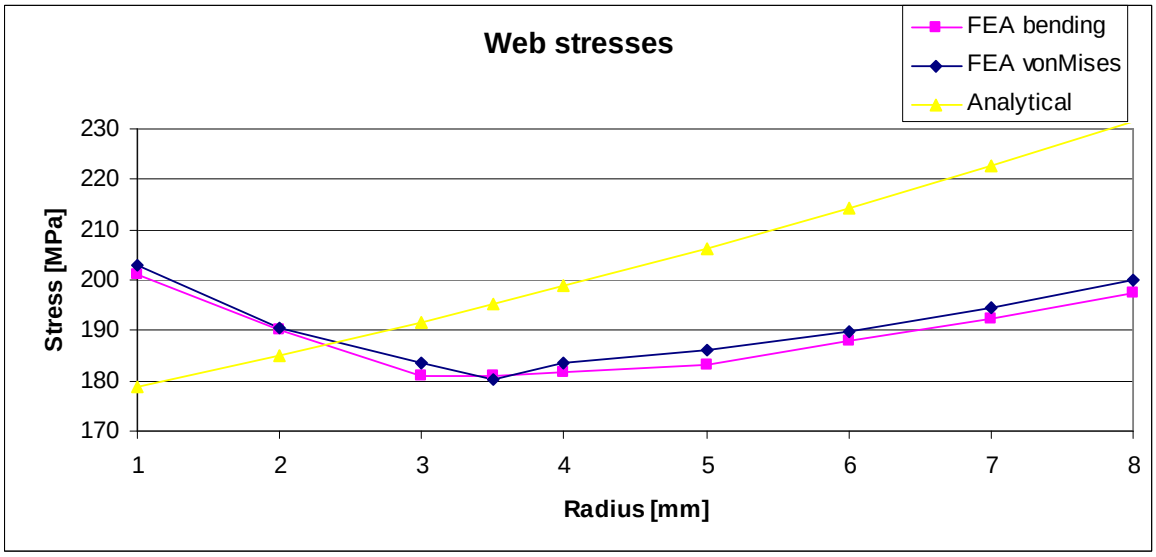

Figure 8.4: Stresses in web for various radii

An additional model with radii of 3.5 mm is analyzed, showing a vonMises peak stress of 180.4 MPa. This confirms the location of the minimum value as indicated by the plot above.

Two effects are shown in the plot above. The peak stresses decrease with increasing radii down to a minimum around 3.5 mm radii due to decreasing stress concentrations. After 3.5 mm the peak stress increase for increasing radii. This is due to a shorter effective length, which creates larger bending moments. The two effects are shown in Figure 8.5 and Figure 8.6 below.

It is also seen that the analytical solutions are higher than the FE results, except for the radii where large stress concentrations occurs. This indicates that the effective lengths used in the analytical calculations are too short. The different slope of the curves also indicate this, as the analytical stresses increase faster than the stresses found in the FE analysis, for increasing radii.

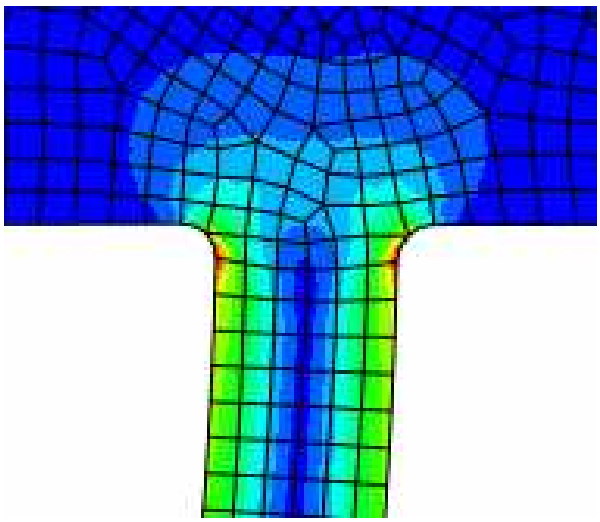

Figure 8.5: Radii 1 mm – Stress concentrations

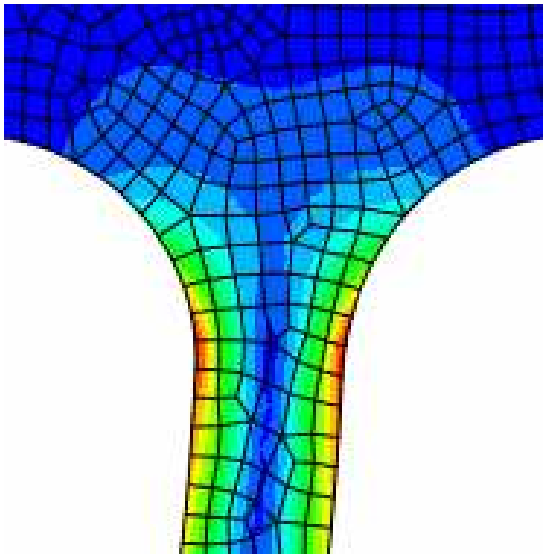

Figure 8.6: Radii 8 mm – Shorter effective length

It is concluded that the optimal radii for this profile subjected to out-of-plane bending is 3.5 mm. There may be a beneficial effect from reducing the radii of the bottom stiffeners. This should however be evaluated closer, since the stresses may increase for other load types where the effective length (height) of the web is irrelevant.

9 FATIGUE ASSESSMENT

This chapter aims to estimate the fatigue life of the modified floating frame structure previously described in a simplified manner. There are several uncertainties in the calculations, and estimates are performed in a conservative manner throughout the assessment.

Since the long term distribution of the stresses is unknown, it is suitable to use an equivalent stress range based on the Weibull distribution. The equivalent stress range obtained can be used directly with a SN-curve, thus predicting the fatigue damage expected. The formula for the equivalent stress range is shown below. (Berge, 2001)

$$\Delta S_{eq} = \frac{\Delta S_0}{(\ln n_0)^{1/h}} \left[\Gamma(1+\frac{m}{h}) \right]^{1/m}$$

ΔS_{eq}: Equivalent stress range
ΔS_0: Maximum stress range in the load history (175 MPa)
n_0: Total number of load cycles in the load history ($5x10^7$)
h: Weibull shape parameter (0.8)
Γ: The complete Gamma function ($\Gamma(1+5.4)=241$)
m: Crack growth exponent (4.32)

For a total life of 20 years, 10^8 cycles is commonly used. This corresponds to almost one load cycle every sixth second for the entire period. For a passenger vessel this would be extremely conservative, since the vessel is not in operation all day and night. The total number of cycles (n_0) is set to $5x10^7$, which still is a conservative estimate.

The Weibull shape parameter is a factor governing the convexity/concavity of the exceedance spectrum. For h-values below 1.0 a concave shape is obtained, while values above 1.0 means a convex shape, as illustrated in Figure 9.1. In this case both slamming loads and pressure fluctuations from waves are considered, in a simplified manner. Since the slamming loads are rare, but with high stress ranges and the pressure fluctuations are common, but with small stress ranges, a concave shape is assumed for the exceedance spectrum. The Weibull shape factor (h) is set to 0.8 as an estimate.

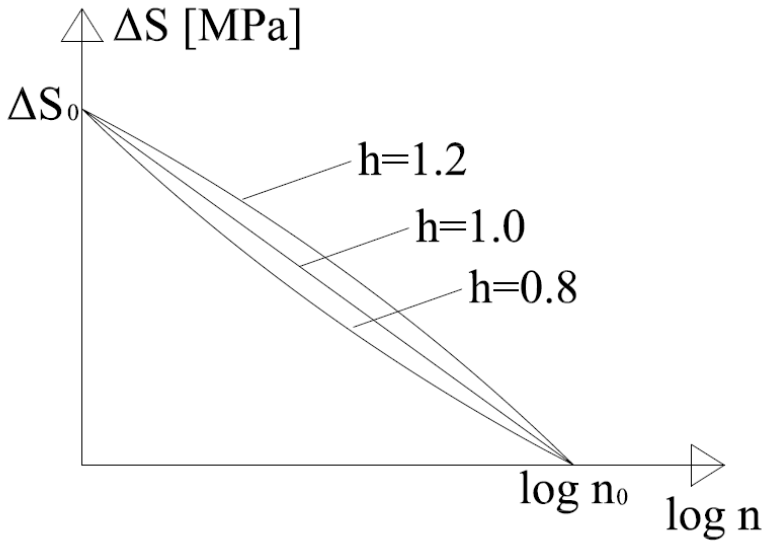

Figure 9.1: Example of Weibull spectrum

The maximum stress range is taken from the stress analysis in chapter 7. Stress concentrations in the range 160-190 MPa are observed. Since some of the stress concentrations are very local, and may originate from mesh deficiencies, the middle value of 175 is chosen as the maximum stress range for fatigue purposes. This should ensure conservatism in the calculations, since nominal stresses normally are assumed for the S-N curves in ECCS Recommendations. (ECCS, 1992)

The equivalent stress range is found to be, ΔS_{eq}=17.1 MPa, when applying the formula and values listed above.

The structural detail is taken as D3 in the ECCS Recommendations, see Figure 9.2. This is a discontinuous longitudinal fillet weld, and the weld category also includes intermittent web-to-flange connections. This detail is analogous to the weld connection between frame web and stiffener flange for the floating frame structure. Ideally several other details should be checked, for instance longitudinal stresses in the stiffeners due to local slamming. However, a full fatigue analysis is not part of the scope in this thesis.

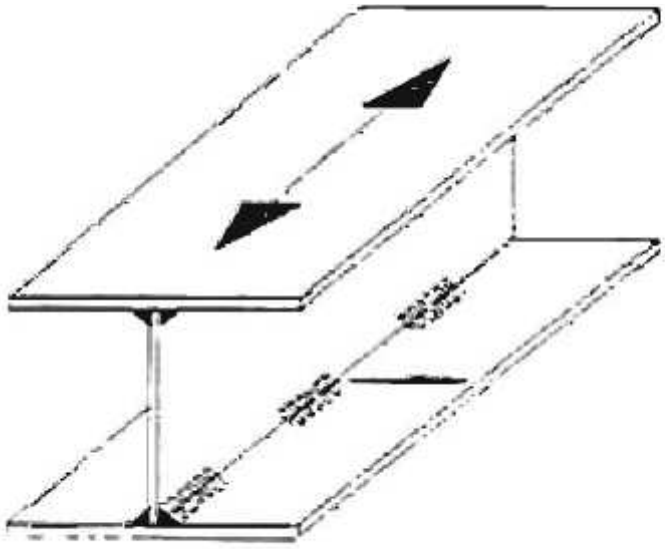

Figure 9.2: Structural detail D3 – ECCS

When comparing the equivalent stress range with the S-N curve for detail D3 in ECCS, which is based on mean minus two standard deviations, the predicted fatigue life of this detail is found to be above $1x10^8$ cycles, which is the largest number of cycles shown in the S-N curve (cut-off limit).

It is found that there is no risk of fatigue failure for this structure within a total life of 20 years, with the assumptions described above. It is however noted that the fatigue assessment in this chapter must only be seen as an estimate, and not a complete fatigue analysis since there are uncertainties related to both load history and choice of detail.

10 NONLINEAR FINITE ELEMENT ANALYSIS

While the FEA in chapter 7 give a good impression of the stresses in the structure, more detailed analyses are required to evaluate the stiffener behaviour in the welded condition. In this chapter nonlinear finite element analyses (NLFEA) are performed in Abaqus to investigate the effect of HAZ for both cyclic loading and ultimate capacity.

Both geometric and material nonlinearities are accounted for, but for the cyclic analyses the geometric nonlinearity are in reality neglectable due to the relatively small deflections. The material nonlinearities are however very central for both analyses, as shown later in the chapter.

The T-profile "T88x5x50x10" is used for this study, which this is a "standard" profile used by Fjellstrand AS. This is also the same profile used for the study in chapter 8, but not the profiles used in the stress analysis in chapter 7. Since the motivation for this study is the nonlinear material properties, and not the exact stresses, this is an acceptable approach.

10.1 Modelling

Due to the complexity of a NLFEA only a limited part of the structure is modelled, as shown in Figure 10.1 below. One stiffener is modelled over 1 m corresponding to one frame spacing. The extent of the shell plate is taken as one stiffener spacing of 235 mm. The edges are given symmetrical boundary conditions, representing a case where the structure is continued over a larger area both longitudinally and transversely. A small plate in the middle of the stiffener represents the transverse frame, since this is of less interest in the analyses. The deflections are prescribed to this plate, thus recreating the real interaction better than if the deflections were added directly to the stiffener.

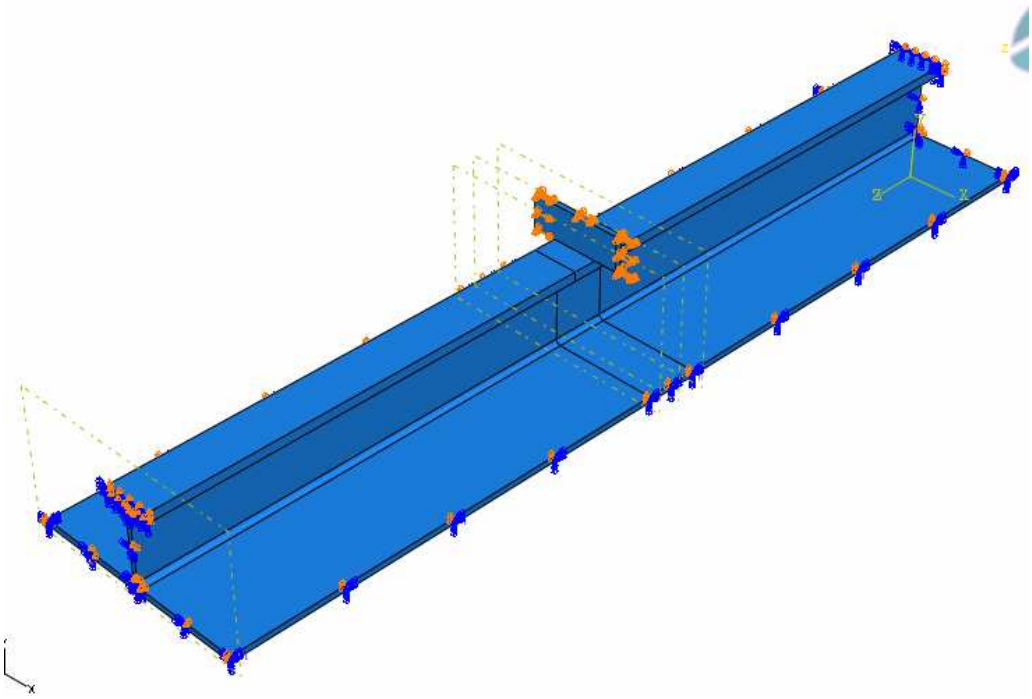

Figure 10.1: Finite element model for nonlinear analyses

For the analyses that include the effect of welding, the extent of the heat affected zones are taken 25 mm in all directions from the weld, as shown in Figure 10.2 below. Since the transverse plate representing the frame is not studied, this is given the original properties of NV-6082.

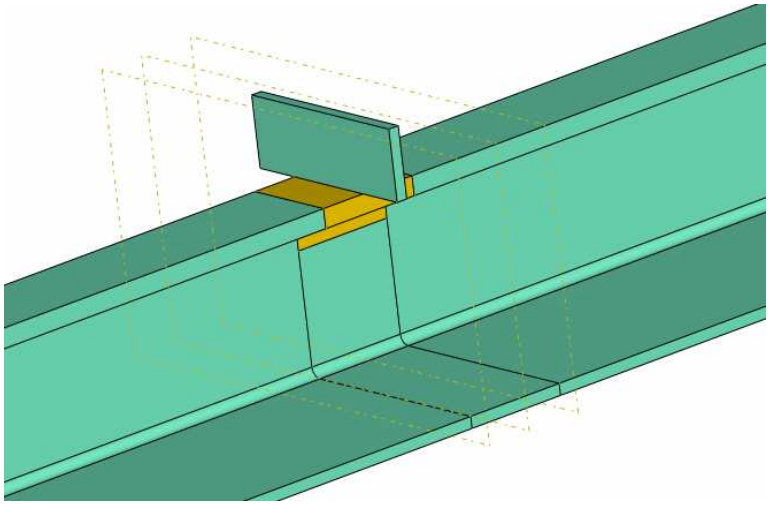

Figure 10.2: Heat affected zones

The element mesh is built up of 4-noded linear tetrahedra, a geometric shape consisting of 4 triangular surfaces. The mesh is quite coarse for most of the model with average mesh size of 12 mm. However, in the areas with HAZ a much more refined mesh is assigned, as shown in Figure 10.3 below. The average mesh size in the refined regions is 1 mm. This is to assure accurate results in the area of most interest. The total number of DOF in the models is ca 41 000.

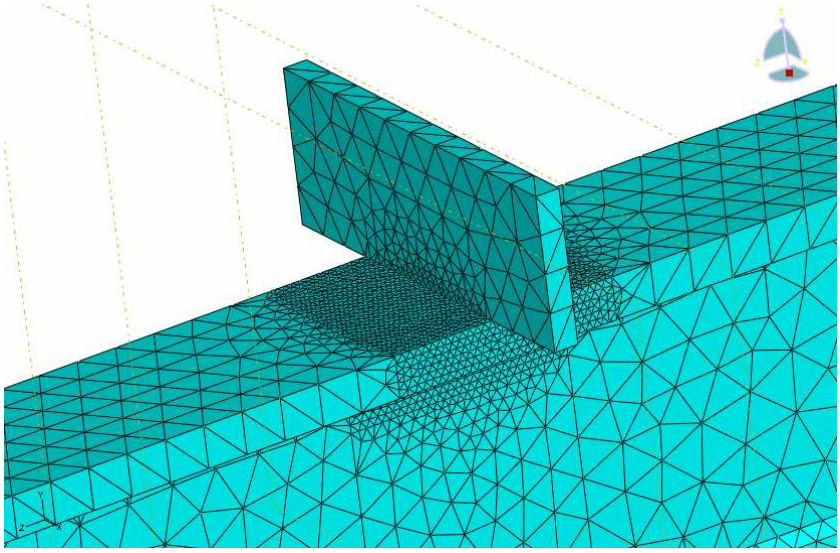

Figure 10.3: Element mesh

10.2 Material Properties

The material data used in this chapter are based on material tests previously performed at the Department for Structural Engineering at NTNU, showing the engineering stress-strain curves for NV-6082 (T6), including the welded properties and NV-5083. Since only the stress-strain curves are available, representative values are manually read off from these curves. Figure 10.4 below shows the engineering stress-strain curves created from the material tests. NV-5083 is in reality used for the frame, but since the frame is not studied in this chapter the plate representing the frame is modelled as NV-6082 for simplicities sake.

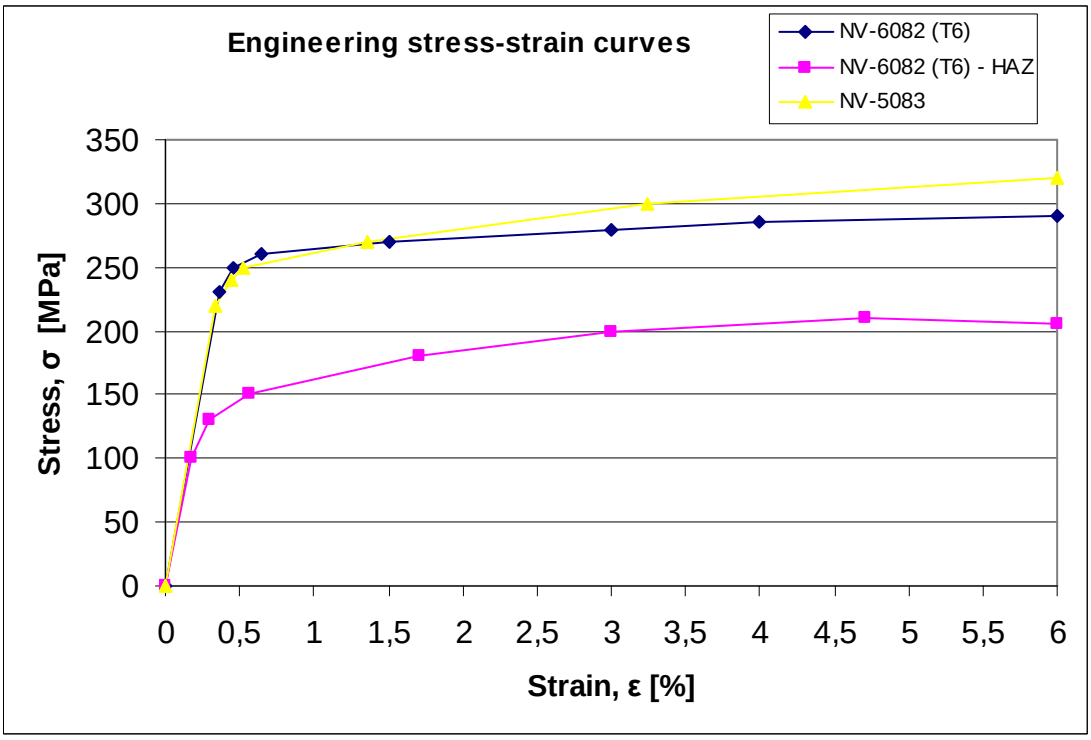

Figure 10.4: Engineering stress-strain curves

It is observed that NV-5083 has a smaller yield value than NV-6082, but display a relatively larger strain hardening than NV-6082. Although this is not directly relevant here it is a useful observation when considering the whole structure.

More relevant for the nonlinear analyses is the relatively large strain hardening for the welded NV-6082 compared to the original material. For strain values of 2 % the heat-affected NV-6082 show a stress level of roughly 70% of the unaffected material. This is large compared to the f_1-values used by DNV in the elastic range. Although the effect of hardening is most pronounced for very large strains, this can be relevant for the ultimate capacity analyses. Substantial hardening (50%) is also observed for strains around 0.5 % for the welded material.

The engineering stresses and –strains are transformed to true stresses and logarithmic strains by using the following relations, since the latter is used as input in Abaqus:

$$\varepsilon_{\ln} = \ln(1+\varepsilon_{eng})$$

$$\sigma_{true} = \sigma_{eng}(1+\varepsilon_{eng})$$

For the strain-hardening input in Abaqus only the plastic strains are used. These are separated from the total strains by subtracting the elastic strains, as shown in Figure 10.5 and the formulae below. (Mathisen, 2009)

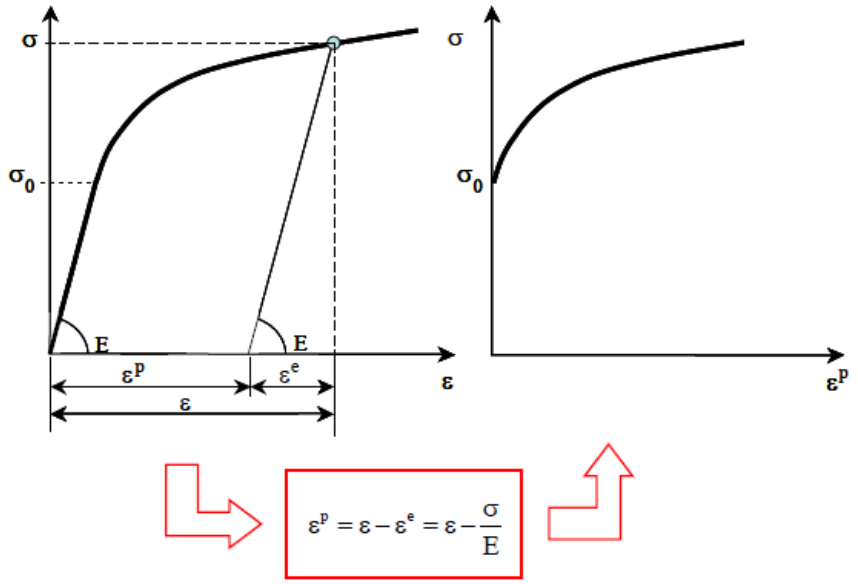

Figure 10.5: Stress-strain relations

$$\varepsilon_{\ln}^{\ pl} = \varepsilon_{\ln}^{\ tot} - \varepsilon_{\ln}^{\ el}$$

$$= \varepsilon_{\ln}^{\ tot} - \frac{\sigma_{true}}{E}$$

The stress-strain data referred to in this chapter and the corresponding input data for Abaqus are shown in appendix V.

An isotropic hardening model is used as input for Abaqus, meaning that the yield surface expands isotropically (symmetrically) about the origin. The choice of hardening model has little influence here, since the loading is not fully reversed.

10.3 Cyclic Analysis

For the cyclic analyses the bottom slamming pressure and a prescribed displacement of 0.56 mm are applied simultaneously in 4 cycles between 100% and 50% as indicated by Figure 10.6 below. The load increment is set to 0.1, meaning that the load and displacement are added/removed stepwise 10% at a time. This gives a total of 80 steps, since each cycle consists of both loading and unloading. The term "time" on the x-axis can be misleading, but is used by Abaqus as an expression for "step". Two steps (time =2) is the same as one cycle.

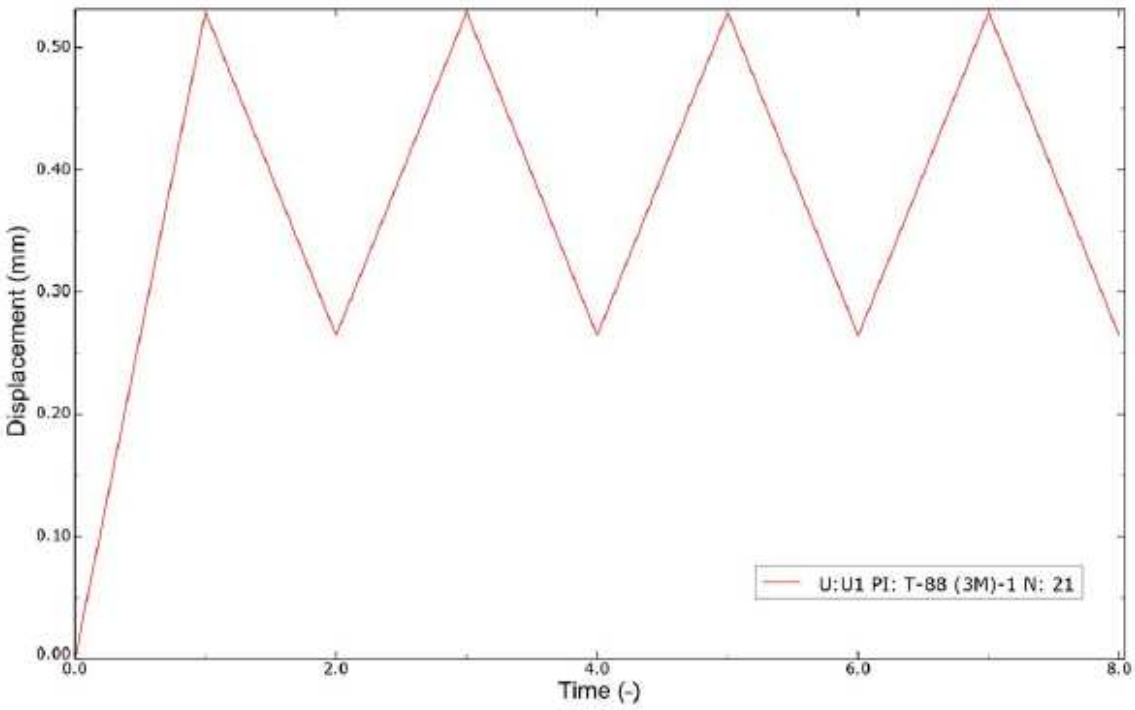

Figure 10.6: Cyclic loading

The displacement value of 0.56 mm is taken from the linear FEA, but since the modelled profile differs from those in the FEA, these analyses can only be taken as examples.

Cyclic analyses are performed both with and without HAZ in the areas previously illustrated. The results from the analyses are shown in form of stress-strain plots in Figure 10.7 below. Total, logarithmic strains have been used.

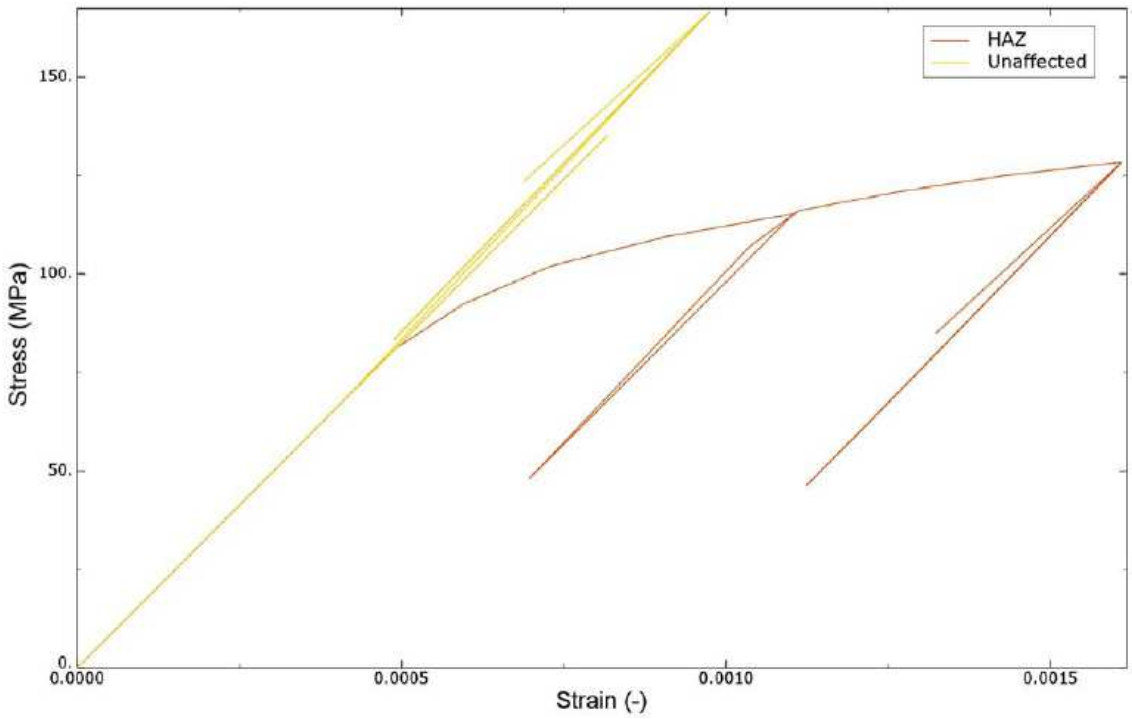

Figure 10.7: Stress-strain plot for cyclic loading

Although there is some numerical noise in the analyses it can be seen that the model unaffected by welding operates solely in the elastic regime, with a complete reversal of the stresses when unloading. The model with heat affected zones, however, is subjected to stresses above yield, and display strain hardening. As the plastic strains develop the yield stress increase, and it is seen that the last two cycles are completely elastic.

The permanent plastic strains are shown in Figure 10.8 below.

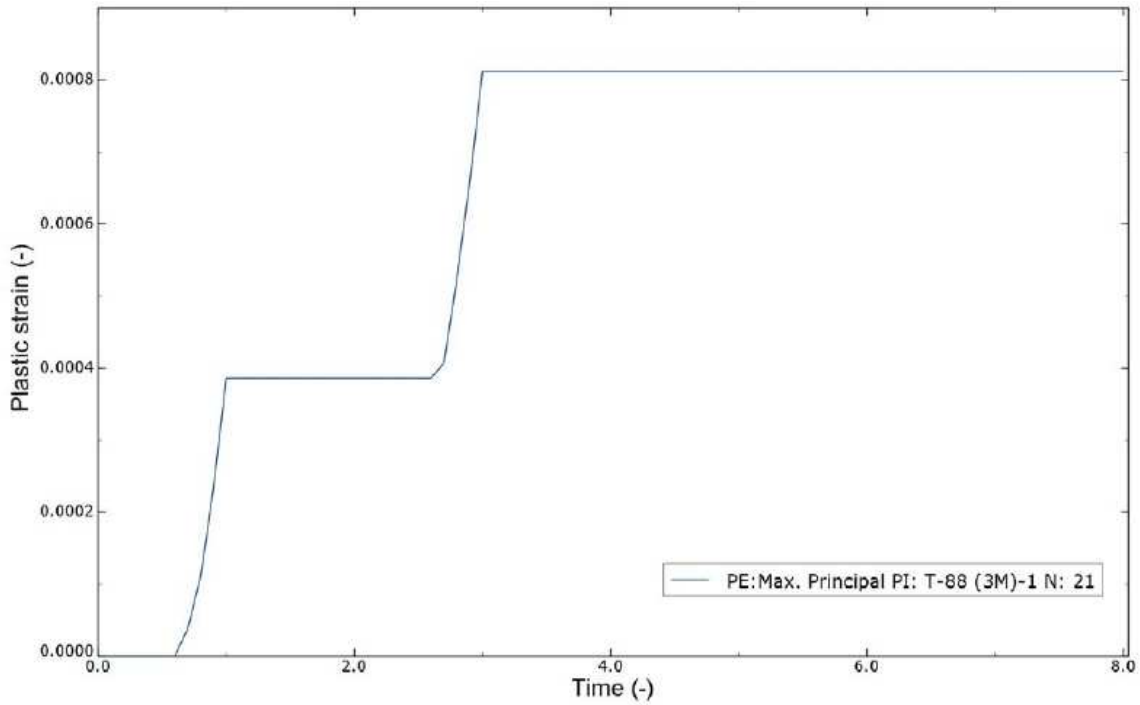

Figure 10.8: Permanent plastic strains

The plastic strains are developed during the first two cycles, and are permanent thereafter. A final plastic strain value of ca 0.08% is found.

Substantial strain hardening is found even for limited strain values (ca 0.16%). This indicates that cyclic loading leading to stresses above the criteria will increase the yield stress for subsequent load cycles. Some of the original material properties have been regained through cyclic loading.

10.4 Ultimate Capacity Analysis

To evaluate the ultimate capacity of the structure and the effect of HAZ, analyses are performed with extreme displacements. In addition to the full slamming pressure a horizontal displacement of 40 mm is prescribed to the structure.

The load increments are again set to 0.1, but due to the larger extent of the analyses the step length is not fixed at that value. This means that Abaqus may increase or decrease the increment based on the number of iterations needed to reach equilibrium in the previous step. A quicker analysis may thus be performed without compromising the accuracy.

The results of the analyses can be seen in the force-displacement (P-Δ) diagram in Figure 10.9 below.

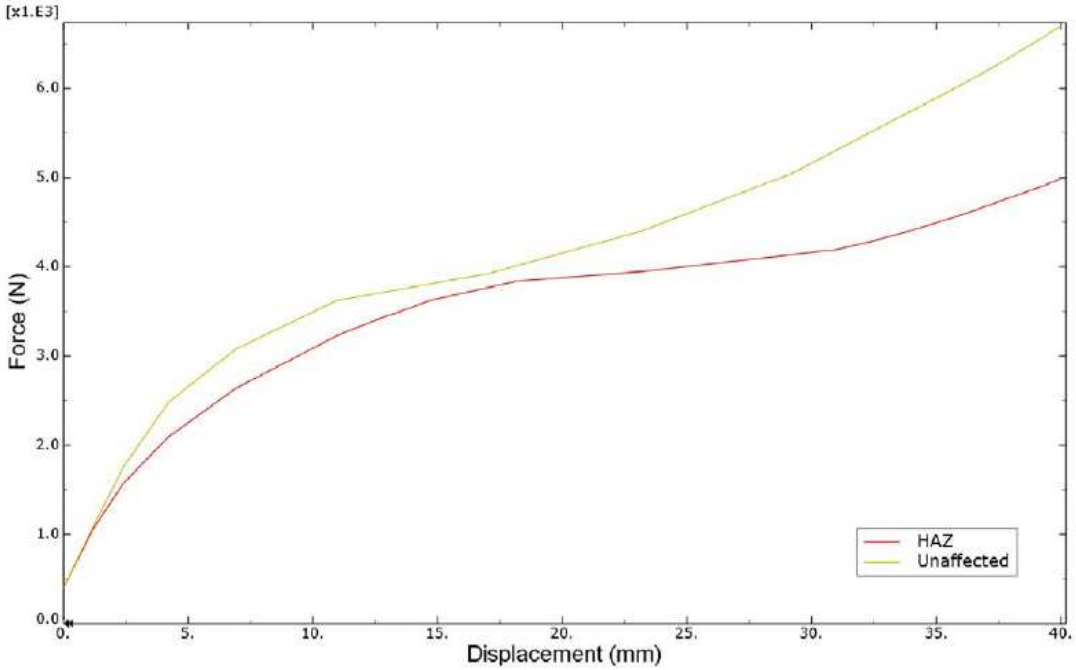

Figure 10.9: Force-displacement curves

The same effects are seen for both the models, although not for the same values. Two effects can be read from the diagram above. First the stiffness of the structure starts to drop at displacements values of 3-4 mm due to yielding, until the middle cross section becomes fully plastic and the stiffness is almost singular. A hinge is then formed and as the displacement continues the stiffness increases due to longitudinal membrane action in the surrounding structure. This redistribution can be seen in the longitudinal view presented in Figure 10.10 below.

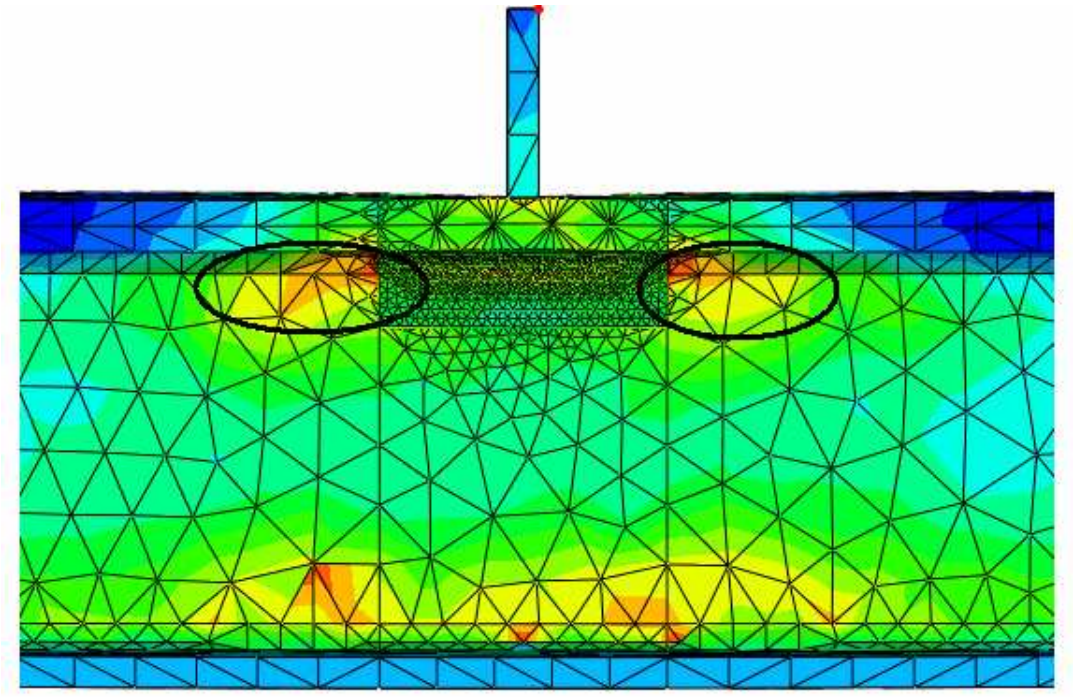

Figure 10.10: Redistribution of stresses after yielding

Due to the lower yield value of the heat affected material, the HAZ model looses its initial stiffness before the unaffected model. Also, a larger hinge is formed which can be seen by the relatively larger segment with almost no stiffness (at around 18-30 mm). At even larger displacements the stiffness of the heat affected model would increase as there seem to be a shift between the two curves. This is partly confirmed by an additional analysis where the heat affected model is displaced 60 mm, as shown in Figure 10.11 below. At this stage the stiffness drops again as yielding starts to take place at the end boundaries.

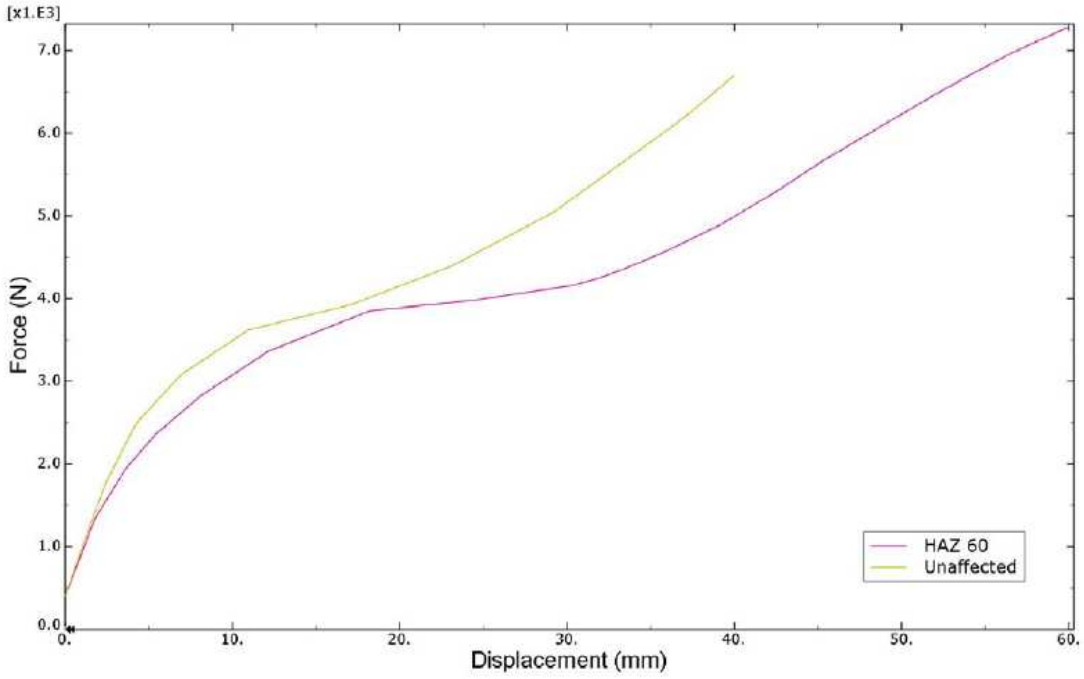

Figure 10.11: Shift in force-displacement curves

The final deformed shape of the two models can be seen in Figure 10.12 below, with the heat affected model to the left. Pronounced hinges are seen for both models.

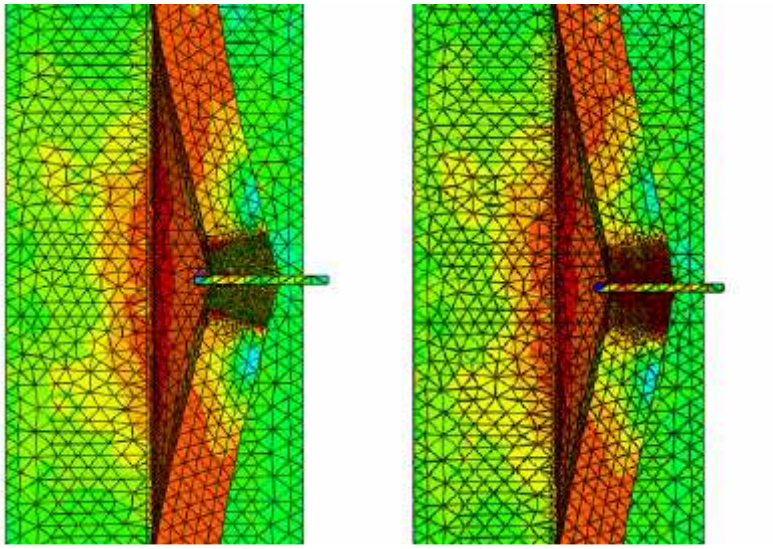

Figure 10.12: Plastic hinges

Due to the forming of plastic hinges there is considerable reserve strength after yielding for the structure, regardless of the local softening in the heat affected zones. It should however be noted that occurring fractures are likely to reduce the effect due to excessive strain levels. At a displacement value of around 30 mm, strains of 8% are observed, suggesting that this might be a more realistic value for the ultimate capacity, as 8% is the elongation value given in DNV HSLC for NV-6082.

11 WEIGHT CALCULATIONS

Of the total cost for building catamarans at Fjellstrand AS the aluminium fabrication cost has previously been calculated to 25%, while the aluminium material cost only amount to 3% of the total cost, according to Stig Oma (Fjellstrand AS).The motivation for the ongoing project "Alubåt" is to come up with more cost-efficient ways to manufacture aluminium hulls, of which the use of floating frames is a possible solution. When applying a floating frame structure the welding time is greatly reduced, since the shell plating and stiffeners are pre-fabricated by extrusion, and only welded to the web frames at the intersections.

The increase in weight when applying a floating frame structure is found to be quite significant. For the bottom structure the frame weight increases with 103% when modifying the frame as described in chapter 6.6. The weight increase for the panels (stiffeners and shell plating) is found to be 6% when complying with the modified DNV HSLC rules outlined in chapter 4.1. This gives a total weight increase of 29% for the bottom structure compared to the original, fixed structure.

11.1 Reduced Stiffener Spacing

While the number of stiffeners in a traditional structure has a large impact on the fabrication cost due to welding time, this is not the case for a floating frame structure. This gives an opportunity to optimize the stiffener spacing with regards to weight, without increasing the fabrication cost to the same degree as for a traditional, fixed structure.

In this chapter the weight of the bottom panel is calculated for various stiffener spacings, while still meeting the requirements in DNV HSLC, with the rule modifications proposed in chapter 4.1. The out-of-plane bending stresses caused by the frame deflections and the proposed interaction formula for bending capacity/contact force are kept out of the calculations, and may prove to limit the potential weight savings to some degree.

The local slamming pressure will generally increase for decreasing stiffener spacing due to a smaller load area. However, in the rules there is a minimum load area of $0.002\Delta/T$ that is already active for the stiffener and plate slamming load, making it even more efficient to reduce the stiffener spacing in this particular case.

The required properties for bottom plating and – stiffeners are shown in Table 11.1 below for 6 different stiffener spacings, with 235 mm as the original spacing, see appendix VI.

Table 11.1: Required properties

Stiffener spacing, s [mm]	Local slamming pressure, p [kN/m^2]	Minimum plate thickness, t_{min} [mm]	Required plate thickness, t_{req} [mm]	Required stiffener shear area, As [cm^2]	Required stiffener sec. modulus, Z [cm^3]
235	149,7	4,7	6,4	5,5	34,6
215	149,7	4,3	5,9	5	31,7
195	149,7	3,9	5,4	4,5	28,7
175	149,7	3,5	4,8	4,1	25,8
155	149,7	3,1	4,3	3,6	22,8
135	149,7	3,1	3,7	3,1	19,9

6 different L-profiles are established based on the requirements above. These are “smeared” to obtain equivalent thicknesses, by dividing the stiffener area by the corresponding stiffener spacing. In Figure 11.1 below, the plate thicknesses, equivalent stiffener thicknesses and total equivalent thicknesses are shown as a function of the stiffener spacing.

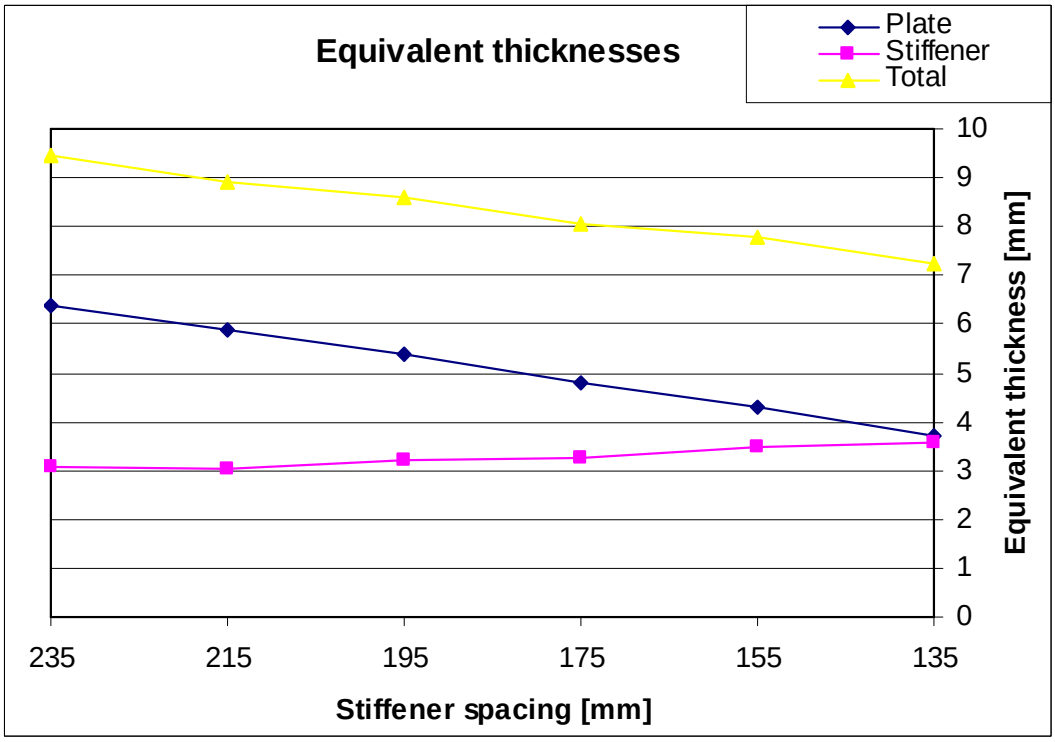

Figure 11.1: Equivalent plate thickness

It is seen that the required plate thickness decreases rapidly for decreasing stiffener spacing. Even though the contribution from the stiffener increase, the total equivalent plate thickness decreases, showing that there is a potential for weight reduction by decreasing the stiffener spacing.

By applying a stiffener spacing of 155 mm a weight reduction of 13% is obtained for the bottom panels. The total weight increase for the bottom structure will then be 15% when including the 103% increase in frame weight. The original weight increase of 29% has almost been bisected by these changes.

Additional considerations should however be taken before reducing the plate thickness drastically. The minimum thicknesses given by the rules may turn out to be too thin in practice, and new problems may arise. Vibrations from the engines should especially be considered, since the engines are located close to the area in question.

12 REFERENCES

Aalberg, Arne (2006a): *Redningsselskapets skøyte "Knut Johan" – konstruert med stivere liggende utenpå spantprofiler*, report, Institutt for konstruksjonsteknikk, Trondheim

Aalberg, Arne (2006b): *Stiver lagt direkte på spant, økt krav til motstandsmoment W for stiveren som følge av konsentrert kraft på oppleggspunktet,* report, Institutt for konstruksjonsteknikk, Trondheim

Amdahl, Jørgen (2006): *Vurdering av lokalkrav til plater og stivere i ulike standarder for småbåter i aluminium,* report, Institutt for marin teknikk, Trondheim.

Berge, Stig (2001): *Fatigue and fracture design of welded structures,* Kompendium, Institutt for marin teknikkk, Trondheim

Det Norske Veritas (2005): *Rules for Classification of High Speed, Light Craft and Naval Surface Craft*, Høvik

Det Norske Veritas (1997): *Tentative Rules for Certification and Classification of Boats*, Høvik

Det Norske Veritas (1996): *Strength Analysis of Hull Structures in High Speed and Light Craft*, Classification Notes 30.8, Høvik

Englund, Jon (2009a): *Structural strength of work boats and high speed crafts with floating frames,* master thesis, KTH Centre for Naval Architecture, Stockholm

Englund, Jon (2009b): *Oppsummering av FE-analyser på Jumbocat 60 med flytande rama,* report for the "Alubåt" project, Oma

European Convention for Construction Steelwork (1992): *European Recommendations for Aluminium Alloy Structures Fatigue Design,* report N° 68, Brussel

European Committee for Standardisation (2004): *ENV 1999-1-1/Eurocode 9: Design of aluminium structures – General structural rules*, Brussels

Mathisen, Kjell Magne (2009): Lecture notes in TKT4197 – Nonlinear Finite Element Analysis, Institutt for konstruksjonsteknikk, Trondheim

Norwegian Maritime Directorate (1990): *Nordic Boat Standard - Commercial Boats less than 15 metres*, Norway

Simulia (2007a): *Abaqus/CAE User's Manual (version 6.7),* Dassault Systèmes, United States

Simulia (2007b): *Abaqus/CAE Theory Manual (version 6.7),* Dassault Systèmes, United States

Økland, Ole David (1999): *Analysis of Transverse Section of the 60m Jumbo Cat*, rapport MT70 F99-390, Marintek, Trondheim

APPENDIX I: DNV HSLC - DESIGN LOADS (PT. 3, CH. 1)

Input

Length, Lpp	54	m
Reduction of Cw (restriction)	0	%
Fully loaded draught, T	2,24	m
Lowest draught, Tl	1,9	m
Number of hulls, n	2	
Displacement fully loaded, Δ	580	t
Maximum speed, V	35	knots
Stiffener spacing, s	0,235	m
Frame spacing, l	1	m
Frame span, S (for slamming area)	3,8	m
Effective frame span, S	3	m
Acceleration of gravity, g	9,81	m/s2
Deadrise angle, βx	13	deg

Sec. 2, B200 - Design vertical acceleration

Acceleration factor from type and restrictions, fg	1	
Design vertical acceleration, acg	4,54	m/s2
Minimum design vertical acceleration, acg	9,81	m/s2

Sec. 2, C201 - Bottom slamming

Long. slamming pressure distr. factor, kl	1	
Draught at L/2 in normal operation condition, T0	2,24	m
Plate area	0,52	m2
Stiffener area	0,52	m2
Frame area	3,8	m2
Slamming pressure on bottom, Psl - plate	149,7	kN/m2
Slamming pressure on bottom, Psl - stiffener	149,7	kN/m2
Slamming pressure on bottom, Psl - frame	82,3	kN/m2

Sec. 2, C203 - Pitching induced bottom slamming

Wave coefficient, Cw	4,32	
ka (plating)	1	
ka (stiffeners/girders)	0,73	
kb (plating/stiffeners)	1	
kb (transverse girders)	0,95	
Slamming pressure on bottom, Psl - plate	116,4	kN/m2
Slamming pressure on bottom, Psl - stiffener	85,0	kN/m2
Slamming pressure on bottom, Psl - frame	80,7	kN/m2

Extent of full pitching slamming (from FP)	29,7	m
Gradually reduced to zero at (from FP)	39,15	m

Sec. 2, C500 - Sea pressure

Longitudinal distr. factor, ks	7,54	(Økland)
a	1	
Location from keel	1	m
Distance from WL, h0	1,24	m
Sea pressure, p	41,4	kN/m2

APPENDIX II: DNV HSLC - HULL STRUCTURAL DESIGN (PT. 3, CH. 3)

(General input taken from sheet "Loads")

Additional input

Radius of curvature, r	4,8	m	
Yield strength, σf (plating/stiffener)	250	Mpa	NV-6082 (T6)
Yield strength, σf (frame)	215	Mpa	NV-5083
Factor f1 (Plating/stiffener - HAZ)	0,48		NV-6082 (T6)
Factor f1 (Frame - HAZ)	0,6		NV-5083

Plating

Basic stiffener spacing, sR	0,308		
s/sR	0,76		
t0 (bottom)	4	mm	
k (bottom)	0,03		
t0 (above WL)	3,5	mm	
k (above WL)	0,02		
f	0,85		

Sec. 5, B101 - Minimum thickness

Minimum thickness, t (bottom)	4,7	mm	
Minimum thickness, t (above WL)	3,8	mm	

Sec. 5, B202 - Bending (Applicable when aspect ratio(s/l) < 0,5)

Sea pressure, p	41,4	kN/m2	(At given location)
Allowable bending stress, σ	86,4	Mpa	(Static - 180*f1)
Thickness requirement, t	3,64	mm	(At given location)

Sec. 5, B302 - Slamming

Slamming pressure on bottom, Psl - plate	149,7	kN/m2	
Allowable bending stress, σsl	96	Mpa	(Dynamic - 200*f1)
Correction factor for curved plates, kr	0,98	-	
Thickness requirement, t	6,41	mm	

Stiffeners

Bending moment factor, m	85		(Continuous longitudinal members)

Sec. 5, C101 - Bending

Allowable bending stress, σ	76,8	Mpa	(Static - 160*f1)
Required section modulus, Z	10,76	cm3	(At given location)

Sec. 5, C201 - Slamming

Slamming pressure on bottom, Psl - stiffener	149,7	kN/m2	
Allowable bending stress, σ	86,4	Mpa	(Dynamic - 180*f1)
Allowable shear stress, τ	43,2	Mpa	(90*f1)
Required section modulus, Z	34,61	cm3	
Required shear area, As	4,2	cm2	(Original formula)
Required shear area, As (floating frames)	5,5	cm2	(Adjusted for floating frames)

Frames

Sec. 6, A301 - Minimum thicknesses

f	0,90		
Basic stiffener spacing, sR	0,308		
s/sR	1,00		
t0	3	mm	
k	0,03		
Minimum thickness, t	4,88	mm	

Sec. 6, A401 - Allowable stresses

Dynamic bending, σ	108	Mpa
Dynamic shear, σ	54	Mpa
Static bending, σ	96	Mpa
Static shear, σ	54	Mpa

Sec. 6, B401 - Strength requirements

Bending moment factor, m	100	(Web frames)
Shear force factor, ks	0,63	(Web frames)

Sea pressure, p	41,4	kN/m2	
Slamming pressure on bottom, Psl - frame	82,3	kN/m2	
Required section modulus, Z (sea pressure)	387,99	cm3	(At given location)
Required section modulus, Z (slamming)	686,10	cm3	
Required shear area, Aw (sea pressure)	14,48	cm2	(At given location)
Required shear area, Aw (slamming)	28,82	cm2	

NOTE: These rules are based on a regular geometry
which is not the case here (for the frames)

APPENDIX III: ANALYTICAL CALCULATIONS OF FRAMES

Input

Effective span (for angles)	2,25	m	
Span, S	3	m	
Pressure, p	82,3	kN/m2	
Stiffener length, L	1	m	
Line load, q	82,3	kN/m	
Youngs modulus, E	70000	Mpa	
Shear modulus, G	26000	Mpa	

Cross-sectional properties

Neutral axis, na	74,1	mm	
Inertia moment, Ixx	1,1E+08	mm4	
Section modulus, bottom	1,5E+06	mm3	
Section modulus, top	4,5E+05	mm3	
Shear area, As	1860,0	mm2	

Moments

Simply supported (middle)	92,59	kNm	
Fixed (ends)	61,73	kNm	
Fixed (middle)	30,86	kNm	
m=10 (case in between - ends)	74,07	kNm	

Stresses

			(Compression)
Simply supported - bottom (middle)	-63	Mpa	(Tension)
Simply supported - top (middle)	205	Mpa	(Tension)
Fixed - bottom (ends)	42	Mpa	(Compression)
Fixed - top (ends)	-137	Mpa	(Compression)
Fixed - bottom (middle)	-21	Mpa	(Tension)
Fixed - top (middle)	68	Mpa	(Tension)
m=10 (case in between) - bottom (ends)	50	Mpa	(Compression)
m=10 (case in between) - top (ends)	-164	Mpa	

Vertical deflections

Simply supported - bending	11,4	mm	
Simply supported - shear deformation	1,9	mm	
Simply supported - total	13,3	mm	
Fixed - bending	2,3	mm	
Fixed - shear deformation	1,9	mm	
Fixed - total	4,2	mm	

Deflection at midpoint, δ	8,7	mm

Angle at end (simply supported)	0,0051	rad

APPENDIX IV: ANALYTICAL CALCULATIONS OF STIFFENERS

Calculations of deflections/stresses for bottom stiffeners

Youngs modulus, E	70000	Mpa	
	Floating	**Modified floating**	
Rotational displacement (frame-FEA), θ:	0,0114	0,0062	rad
Distance to neutral axis (frame), y:	205	211	mm
Web height, L:	84,5	84,5	mm
Web thickness, t:	3,5	3,5	mm
Maximum deflection, Δ:	2,34	1,31	mm
Maximum bending stress, σ:	240,6	134,7	Mpa

Calculations of deflections/stresses for side stiffeners

Unbalanced force, F_unb:	82000	N			
Youngs modulus, E	70000	Mpa			
	"bulb-65"	**test 1**	**test 2**		
Web height, L:	50	55	50		mm
Web thickness, t:	3,5	3,5	4		mm
Effective breadth, b:	400	400	400		mm
Number of stiffeners:n	17	17	17		[ ]
Spring stiffness, k:	9604	7216	14336		N/mm
Total stiffness, K_tot:	163268	122666	243712		N/mm
Average deflection, Δ:	0,50	0,67	0,34		mm
Average bending stress, σ:	147,7	162,4	113,1		Mpa

Stresses proportional to L and 1/t^2
as found by formulae

APPENDIX V: NONLINEAR MATERIAL PROPERTIES

Youngs modulus, E 70000 Mpa

NV-6082 (T6)

Yield (DNV) = 250 Mpa

ε_eng [%]	ε_eng [-]	σ_eng [Mpa]	ε_ln [-]	(Input Abaqus) σ_true [Mpa]	(Input Abaqus) ε_ln_pl [-]
0	0	0	0	0	
0,36	0,0036	230	0,0036	230,8	0,0000
0,46	0,0046	250	0,0046	251,2	0,0010
0,64	0,0064	260	0,0064	261,7	0,0026
1,5	0,0150	270	0,0149	274,1	0,0110
3	0,0300	280	0,0296	288,4	0,0254
4	0,0400	285	0,0392	296,4	0,0350
6	0,0600	290	0,0583	307,4	0,0539

NV-6082 (T6) - HAZ

Yield (DNV) = 120 Mpa

ε_eng [%]	ε_eng [-]	σ_eng [Mpa]	ε_ln [-]	(Input Abaqus) σ_true [Mpa]	(Input Abaqus) ε_ln_pl [-]
0	0	0	0	0	
0,18	0,0018	100	0,0018	100,2	0,0000
0,29	0,0029	130	0,0029	130,4	0,0010
0,57	0,0057	150	0,0057	150,9	0,0035
1,71	0,0171	180	0,0170	183,1	0,0143
3	0,03	200	0,0296	206,0	0,0266
4,71	0,0471	210	0,0460	219,9	0,0429
6	0,06	205	0,0583	217,3	0,0552

NV-5083

Yield (DNV) = 215 Mpa

ε_eng [%]	ε_eng [-]	σ_eng [Mpa]	ε_ln [-]	(Input Abaqus) σ_true [Mpa]	(Input Abaqus) ε_ln_pl [-]
0	0	0	0	0	
0,34	0,0034	220	0,0034	220,7	0,0000
0,45	0,0045	240	0,0045	241,1	0,0010
0,53	0,0053	250	0,0053	251,3	0,0017
1,36	0,0136	270	0,0135	273,7	0,0096
3,24	0,0324	300	0,0319	309,7	0,0275
6	0,06	320	0,0583	339,2	0,0534
8	0,08	330	0,0770	356,4	0,0719

APPENDIX VI: PANEL WEIGHT FOR REDUCED STIFFENER SPACING

Requirements:

Spacing	p	t_min	t_req	As	Z
235	149,7	4,7	6,4	5,5	34,6
215	149,7	4,3	5,9	5	31,7
195	149,7	3,9	5,4	4,5	28,7
175	149,7	3,5	4,8	4,1	25,8
155	149,7	3,1	4,3	3,6	22,8
135	149,7	3,1	3,7	3,1	19,9

Dimensions:

Spacing	235	215	195	175	155	135	mm
Plate thickness, tp	6,4	5,9	5,4	4,8	4,3	3,7	mm
a/b	2,6	2,8	3,1	3,4	3,9	4,4	
C (from table)	0,76	0,8	0,85	0,87	0,92	0,94	
Effective width, be	179	172	166	152	143	127	mm
Web thickness, tw	5	4,5	4,5	4,1	4	3,5	mm
Web height, h	100	100	90	90	80	80	mm
Flange thickness, tf	10	10	10	10	10	10	mm
Flange width, bf	22	20	22	20	22	20	mm

Neutral axis, na	30,25	30,23	29,55	30,84	30,47	32,48	mm
Inertia moment, Ixx	3,0,E+06	2,7,E+06	2,2,E+06	1,9,E+06	1,5,E+06	1,3,E+06	mm4
Section modulus, bottom	100792,5	90399,7	74554,6	62476,6	48825,8	38770,8	mm3
Section modulus, top	35398,9	31900,5	29044,6	26055,6	23310,5	20573,6	mm3
Shear area, As	550,0	495,0	450,0	410,0	360,0	315,0	mm2
Total area, Atot	720,0	650,0	625,0	569,0	540,0	480,0	mm2

Weight:

Aluminium density: 2700 kg/m3

Spacing	235	215	195	175	155	135	mm
Plate thickness	6,4	5,9	5,4	4,8	4,3	3,7	mm
Eq thickness stiffener	3,1	3,0	3,2	3,3	3,5	3,6	mm
Total equivalent thickness	9,5	8,9	8,6	8,1	7,8	7,3	mm

(without frame)

Weight pr m2	25,6	24,1	23,2	21,7	21,0	19,6	kg

(without frame)